THERMODYNAMIC CHARACTERIZATION OF CONFORMATIONAL STATES OF BIOLOGICAL MACROMOLECULES USING DIFFERENTIAL SCANNING CALORIMETRY

Authors: **Rodney L. Biltonen**
Ernesto Freire
Departments of Pharmacology and Biochemistry
University of Virginia School of Medicine
Charlottesville, Virginia

Referee: John F. Brandts
Department of Chemistry
University of Massachusetts
Amherst, Massachusetts

INTRODUCTION

Conformational changes of biological macromolecules play a major role in discussions about the functioning of complex biochemical systems. Abrupt changes in the catalytic activity of enzymes with temperature have been ascribed to reversible, "all-or-none" transitions in the structural state of the macromolecule. Allosteric regulation has been rationalized in terms of ligand-induced conformational changes in proteins. More recently, it has been demonstrated that transfer ribonucleic acids undergo a sequence of conformational changes as a function of temperature and magnesium and salt concentration; these variations in structure may play a role at the various stages of protein synthesis in which tRNA is involved. It has also been suggested that gel-to-liquid crystalline transitions of the phospholipid matrix of biological membranes may play an important role in the functioning of these complex systems.

In order to develop a complete understanding of biological phenomena in molecular terms, it is necessary to identify the structural and thermodynamic characteristics of the accessible states of the system of interest. This review will consider experimental and analytical methods by which identification of the number of accessible states and their thermodynamic characteristics can be made. First, the problems involved in developing a detailed thermodynamic description of conformational transitions of macromolecular systems will be briefly stated. There will follow a description of the basic principles involved in using differential scanning calorimetry to obtain heat-capacity data and a review of the thermodynamic information which has been obtained for a number of systems. It appears, however, that heat-capacity data contain substantially more information relating to the statistical thermodynamic descriptions of complex macromolecular systems than has been normally extracted. Therefore, the last part of this review will consist of a discussion of analytical protocols to obtain such information, as recently developed in the authors' laboratory.

GENERAL CONSIDERATIONS OF MACROMOLECULAR CONFORMATIONAL TRANSITIONS

The major problem in defining the thermodynamic details of a conformational transition of a macromolecule in solution is that the transition may proceed through a series of distinct states, and identification of the number of accessible states and their related thermodynamic parameters is difficult at best. Consider the sequential reaction scheme

$$I_0 \rightleftharpoons I_1 \rightleftharpoons I_2 \text{ ---- } I_{n-1} \rightleftharpoons I_n \qquad (1)$$

where a macromolecule undergoes a transition from some initial state, I_0, to some final state, I_n. The equilibrium situation can be defined by the set of equilibrium constants,

$$K_i = \frac{[I_i]}{[I_{i-1}]} \quad (i = 1, 2, 3 \ldots n) \qquad (2)$$

with which a partition function can be defined as

$$Q = 1 + K_1 + K_1K_2 + K_1K_2K_3 + \text{----} + K_1K_2 \text{ --- } K_n \qquad (3)$$

This partition function is defined in terms of the probabilities of each state relative to that of state I_0 being equal to one at all temperatures.

Before proceeding, it may be useful to make some fundamental definitions. By "state" is meant a macroscopic distribution summed over a number of microstates whose average energy quantities are defined by G°_i, H°_i, S°_i, $C^\circ_{p,i}$, etc. These macrostates are not necessarily static, structurally well-defined entities; they may represent dynamic, fluctuating molecular distributions (e.g., the "native" state of a protein). The transitions between states are reversible in a thermodynamic sense and, from an experimental point of view, are in equilibrium. The enumeration of states makes no implication regarding the kinetic path for transformation. The designation of a state simply means that at some point in the transition it is significantly populated. It should also be noted that this reaction scheme, as well as the derived partition function, is general. The individual states are separated in a sequential sense in terms of increasing enthalpy values. A special case of this representation is a reaction scheme of independent two-state transitions.

The discreteness of the states depends, from an experimental point of view, upon their separation in terms of ΔH_i and ΔS_i. As will be seen in the case of proteins and transfer ribonucleic acids, ΔH_i and ΔH_{i+1} may differ by 30 kcal/mol or more. In other cases, adjacent states will thermodynamically differ very little and will tend to merge so as to form a continuum. This is the case for helix-coil transitions of polypeptides and synthetic ribonucleic acids. A pictorial representation of these differences as they manifest themselves in the energy distribution function is given in Figure 1.

The probability or fractional occupancy, F_i, of each macrostate is given by

$$F_i = \frac{e^{-\Delta G_i/RT}}{Q} \qquad (4)$$

where $\Delta G_i = G^\circ_i - G^\circ_o$. If we assign the value α_i to any general property of state, the average value (measured value) is given by

$$\langle \alpha \rangle = \Sigma \alpha_i F_i = \frac{\Sigma \alpha_i e^{-\Delta G_i/RT}}{Q} \qquad (5)$$

Experimentally, however, one is primarily concerned with changes in an observable relative to that found in some reference state which we will

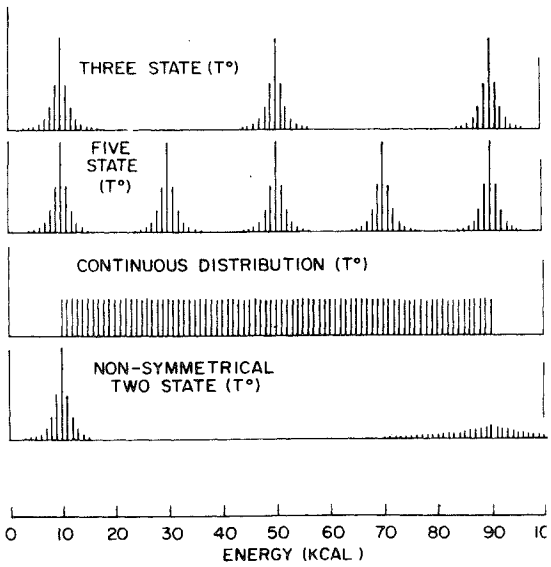

FIGURE 1. Distribution functions for the three-state five-state, uniform-continuous, and nonsymmetrical two state cases at the transition temperature. (From Lumry, R. Biltonen, R., and Brandts, J., *Biopolymers,* 4, 917, 1966 With permission.)

take to be I_0. Thus, we shall define $\Delta\alpha_i = \alpha_i - \alpha_o$ and

$$<\Delta\alpha> = \frac{\Sigma\Delta\alpha_i\, e^{-\Delta G_i/RT}}{Q} \quad (6)$$

If the enthalpy of the system is considered to be the observable, then the excess enthalpy is defined as

$$<\Delta H> = \frac{\Sigma\Delta H_i e^{-\Delta G_i/RT}}{Q} \quad (7)$$

Usually, a general observable is monitored to characterize a transition. This function contains 3 (n−1) parameters ($\Delta\alpha_i$, ΔH_i, and ΔS_i for each step). An advantage of the use of ΔH as the observable is that it is contained as both a coefficient and a parameter in the exponential terms. Thus, only 2 (n − 1) parameters are required to exactly define the transition.

Another advantage of using ΔH as the observable is that its temperature derivative can be directly measured, adding greater sensitivity to the analysis. This derivative is, by definition, equal to the excess heat capacity, $<\Delta C_p>$, and related to the variance of the enthalpy distribution function:

$$<\Delta C_p> = \left(\frac{\partial <\Delta H>}{\partial T}\right)_p = \frac{<\Delta H^2> - <\Delta H>^2}{RT^2} \quad (8)$$

These facts form the basis of the use of differential scanning calorimetry in monitoring macromolecular conformational transitions and the basis for the method of analysis described in this review.

DIFFERENTIAL SCANNING CALORIMETRY

In this review, the applications of the technique of differential scanning calorimetry in the study of conformational changes of biological macromolecules will be considered. The operational details of the technique, however, will not be examined; a number of recent reviews dealing with this aspect of the problem are recommended to the reader instead.[1-3] Nevertheless, it will be useful to briefly consider the basic principles of the measurement before beginning a discussion of the analysis of experimental results.

The traditional differential scanning calorimeter consists of a sample and a reference calorimetric cell which, ideally, are thermally isolated from one another and from the environment. If the cells (including contents) are identical, constant and identical power input into each will produce a constant temperature rise with time in the two cells. This is usually accomplished by placing two identical resistance heaters in series in each of the cells. The rate of temperature rise, γ, is given by[4]

$$\gamma = P/C = I^2R/C \quad (9)$$

where I is the constant current applied to each heater of resistance, R, and C is the heat capacity of each cell in joules per degree.

If the heat capacity of, for example, the sample cell is greater than that of the reference cell, the temperature of the former will tend to lag behind the latter. In order to maintain γ constant in both cells, a temperature-sensing device monitors the temperature difference between the two cells, and, via a feedback circuit, sufficient additional power is applied to an auxiliary heater in the cell which is lagging to null this temperature difference. Thus,

$$\gamma = \frac{P}{C} = \frac{P + \Delta P}{C + \Delta C} \quad (10)$$

and $\Delta C = \Delta P/\gamma$. ΔP is the instantaneous power input via the auxiliary heater in the cell with the greater heat capacity ($C + \Delta C$). Measurement of the absolute temperature (as a function of time) and of ΔP provides the basic information which can be converted to an excess heat capacity vs. temperature function.

The calorimeters designed by Ackermann,[1] Brandts,[6] Gill,[7] Privalov,[8] and co-workers operate in this manner. Sturtevant's calorimeter[9] measures the integrated power input as a function of temperature, which, upon differentiation, yields the excess heat capacity. More recently, Ross and Goldberg[10] designed a calorimeter in which the primary signal is the temperature difference between cells (feedback control is not utilized). This type of calorimeter does not directly yield ΔC, but appropriate computer analysis of the data, as developed by Suurkuusk and co-workers,[11] provides estimates of ΔC as a function of temperature.

In this latter type of calorimeter, based on the heat-leak principle, the two cells are contained within a heat sink. The heat sink, whose heat capacity is much greater than the sample or reference cell, is heated at a constant rate, ideally. Because of thermal barriers between the cells and the sink, the cell temperature, T_c, lags behind that of the sink, T_s. Under steady-state conditions, the rate of heat flow into both cells is proportional to this temperature difference:

$$\frac{dQ}{dt} = K\,(T_S - T_c) \tag{11}$$

where K is a constant of the calorimeter which can be experimentally determined, and

$$C = \frac{dQ}{dT_c} = \frac{dQ}{dt} \Big/ \frac{dT_c}{dt} = \frac{K(T_S - T_c)}{\gamma} \tag{12}$$

(under steady-state conditions, $\gamma = dT_s/dt = dT_c/dt$). If the heat capacity of both cells is identical, no temperature difference between the two cells exists, but if the heat capacity of one is greater by an amount ΔC, then a temperature difference

$$\delta T = \Delta C \frac{\gamma}{K} \tag{13}$$

between the two cells is developed. Thus, monitoring δT and the temperature as a function of time and knowing K, one can determine the excess heat capacity. It is to be noted, however, that because of thermal impedance in the measuring devices which form the thermal barriers, a time-response correction must be made. This correction is straightforward, and its application to yield ΔC as a function of temperature has been discussed by Suurkuusk et al.[11]

The design, construction, and use of calorimeters of the type described above are not implied to be simple. Calorimeters of the necessary sensitivity and precision require rather sophisticated control, monitoring, and data acquisition equipment. For example, the thermal characteristics of cells can never be made identical; cells cannot be isolated from the environment at adiabatic conditions; and, in the case of the heat-leak type calorimeter, extensive computer calculation is required to transform the basic data into a heat-capacity curve.

It should be noted that this discussion will be very concerned about the exact shape of heat-capacity curves obtained with quite small amounts of biological material. For the most part, the only calorimeters capable of generating the required data are those which have been produced in research laboratories throughout the world. The only commercially available calorimeter which meets the necessary requirements is one based on the design of Privalov.[8]

EXCESS HEAT CAPACITIES

For a homogeneous macromolecular system characterized in terms of the Gibbs energy, enthalpy, etc., the excess enthalpy is defined in Equation 7 and given as

$$\langle \Delta H \rangle = H(T) - H_o(T) = \frac{\Sigma \Delta H_i e^{-\Delta G_i / RT}}{Q} \tag{14}$$

where H(T) is the standard enthalpy of the system at temperature T and $H_o(T)$ is the standard enthalpy of the system if it existed in the reference molecular state at temperature T. Thus, the excess heat capacity is

$$\langle \Delta C_p \rangle = \frac{dH(T)}{dT} - \frac{dH_o(T)}{dT} \tag{15}$$

$$= C_p(T) - C_{p,o}(T) \tag{15a}$$

where $C_p(T)$ and $C_{p,o}(T)$ have meanings analogous to H(T) and $H_o(T)$. These definitions are important in all the following discussions; a simple two-state transition will be used to exemplify their significance.

A two-state transition is one in which the macromolecule exists in only two accessible macroscopic states,[12] i.e., the total population of molecules can be accounted for in terms of the occupancy of only two states. In such a situation, the equilibrium $A \rightleftharpoons B$ is described by an equilibrium constant

$$K = [B]/[A] \tag{16}$$

The reference state is taken to be pure state A. The fraction of molecules in state B, F_B, is

$$F_B = \frac{K}{1 + K} \tag{17}$$

In this case, the partition function is $Q = 1 + K$, and all thermodynamic quantities can be derived from it in the normal fashion. The total enthalpy of the system is

$$H(T) = F_A H_A(T) + F_B(H_A(T) + \Delta H(T)) \tag{18}$$

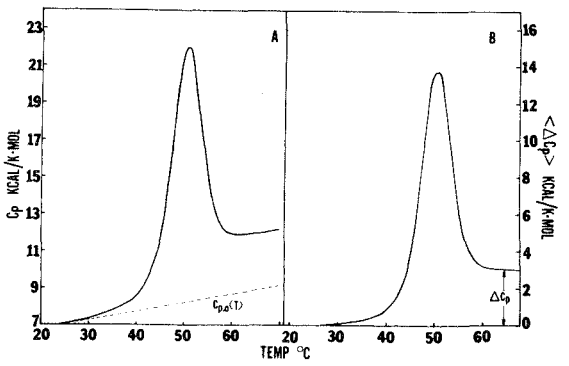

FIGURE 2. Computer-simulated heat capacity function, C_p, and excess heat capacity function, $\langle\Delta C_p\rangle$, for a two-state transition characterized by the following parameters: ΔH = 100 kcal/mol; T_m = 50°C; ΔC_p = 3 kcal/K/mol; $\langle\Delta C_p\rangle$ is obtained from C_p after subtraction of $C_{p,o}$ (dotted line), the heat capacity of the initial state.

where $\Delta H(T) = H_B(T) - H_A(T)$. Noting that $F_A + F_B = 1$, it follows that

$$H(T) = H_A(T) + F_B \Delta H(T) \tag{19}$$

$$\langle \Delta H \rangle = F_B \Delta H(T) \tag{20}$$

and

$$\langle \Delta C_p \rangle = F_B \Delta C_p + \Delta H(T) \frac{dF_B}{dT} \tag{21}$$

The latter term in Equation 21 is referred to as a "between states" heat capacity (arising from a change in the relative population of macroscopic states with temperature), whereas $C_{p,A}(T)$ or $C_{p,B}(T)$ is a "within states" heat capacity (an intrinsic property of a particular macroscopic state), and $\Delta C_p = C_{p,B} - C_{p,A}$.

In an ideal differential scanning calorimeter, the measured quantity is $C_p(T)$, as shown in Figure 2A, for a hypothetical two-state transition. In order to obtain $\langle\Delta C_p\rangle$, it is necessary to estimate the temperature dependence of $C_{p,o}(T)$, as indicated by the broken line. Subtraction of $C_{p,o}(T)$ will yield $\langle\Delta C_p\rangle$, as shown in Figure 2B. This calculated result can then yield estimates of the transition temperature; where $F_A = F_B = \frac{1}{2}$ in the present case, $\Delta H(T) = \int_{T_o}^{T_f} \langle\Delta C_p\rangle \, dT$ and ΔC_p, as indicated in the figure.

This method of estimating the enthalpy change for the transition is extremely important. If one uses the $\langle\Delta C_p\rangle$ curve as defined, the integral provides the enthalpy difference between state B and state A at temperature T_f. If, however, the heat-capacity curve is integrated using the temperature-independent line (solid) shown in Figure 2A, the estimate of ΔH refers to the enthalpy difference between state B at temperature T_f and state A at temperature T_o. This is not particularly important if the transition occurs over an interval of a few degrees but is a serious problem if the transition is broad. Examples of this problem will be viewed later.

A REVIEW OF PREVIOUS CALORIMETRIC STUDIES

The most obvious advantage of scanning calorimetry is that it provides a direct estimate of the overall enthalpy change of a transition without requiring knowledge of the thermodynamic mechanism. Other methods which monitor the transition can provide reasonable estimates of the transition temperature ($\Delta G^\circ \sim 0$), but, unless the reaction is of the two-state type, thermodynamic quantities can only be approximated, at best. In this section, the literature through about 1977 on scanning calorimeter results will be reviewed. These works report the enthalpy changes associated with the double-single strand transition of DNA and some synthetic polynucleotide systems, the gel-liquid crystalline transitions of phospholipid bilayers, and the thermal unfolding of transfer ribonucleic acids; the evaluation of theoretical parameters associated with transitions in homopolymers; and the testing of the two-state hypothesis of the thermal unfolding of globular proteins. It has only been rather recently that analysis of the detailed shape of $\langle\Delta C_p\rangle$ curves for biological macromolecules has been attempted. This recapitulation of past work should provide the background for the discussion to be presented in later sections.

Deoxyribonucleic Acids (DNA)

The double-strand single-strand transition of naturally occurring DNA has been particularly interesting to the calorimetrist. Not only is the system biologically important, but the transition is extremely abrupt and occurs with a large enthalpy change. Thus, it is relatively easy to monitor the transition with most differential

TABLE 1

Thermodynamic Parameters Associated with the Melting Transition of Natural DNA at Neutral pH

DNA	%GC[a]	ΔH[b]	T_m (°C)	Salt concentration	Ref.
T_2 Phage	34	9.65	84.8	0.14 *M* Na^+	13
	34	9.42	81.2	0.087*M* Na^+	13
	34	9.28	75.0	0.044*M* Na^+	13
	34	9.14	71.5	0.029*M* Na^+	13
	34	9.15	66.0	0.015*M* Na^+	13
	34	8.9	64.0	0.011*M* Na^+	13
Cl. perfringens	31	7.73	55.0	0.001*M* K^+	50
M. lysodeikticus	72	8.52	79.0	0.001*M* K^+	50
Salmon sperm	41	7.84	60.6	0.001*M* K^+	50

[a] Content of guanine-cytosine GC base pairs %.
[b] kcal/mol of base pairs.

scanning calorimeters. Unfortunately, the transition is not easily reversible since many "mismatched" aggregates of the heterogeneous single-stranded forms easily assemble. Thus, while the total enthalpy change can be measured, an equilibrium C_p cannot be well defined. Nevertheless, precise values of $\Delta H \simeq 9$ kcal/mol base pairs have been obtained under a variety of conditions. These results, summarized in Table 1, allow the evaluation of the overall energy changes for the transition and provide the basis for estimating the thermodynamic stability (ΔG°) of the DNA double helix in aqueous solution under various conditions, as has been discussed by Privalov et al.[13]

Polypeptides

Homogeneous polypeptides undergo reversible helix-coil transitions as a function of temperature. The enthalpy change for these polymers is not as large as that found for DNA. Nevertheless, the transitions are very cooperative and sensitive to solvent condition; in water, the temperature-induced transition is from helix to coil form, whereas in certain polar, nonaqueous solvents, the transition is from coil to helix form as the temperature is raised. The application of differential scanning calorimetry has allowed the evaluation of enthalpy changes for a limited number of systems. These results are tabulated in Table 2.

Although the detailed shape of C_p curves of polypeptides has not been analyzed, Ackermann and Newmann[14] have evaluated the basic data in theoretical terms for transitions of topologically one-dimensional systems. The theory of Zimm and Bragg[15] states that the transition in an infinite-sized polypeptide can be described in terms of three parameters: Δh_c, Δs_c, and σ. Δh_c is the enthalpy change per residue, Δs_c the entropy change per residue, and σ a parameter defining the degree of cooperative interaction between residues. $\Delta g_c = \Delta h_c - T\Delta s_c$ is equal to the free-energy change associated with the addition of a single helical residue to an already existing helical segment.

A typical C_p curve for a polypeptide transition is shown in Figure 3. The extrapolated baseline heat capacity is shown as a broken line. This extrapolation assumes that ΔC_p for the transition is zero. Although this may not be exactly correct, the error introduced by this approximation does not seriously affect the analysis. The area under this curve is equal to Δh_c, and $\Delta s_c = \Delta h_c / T_m$ where T_m is identified with the maximum in the heat-capacity curve. Assuming that $\langle \Delta H \rangle$ is linearly related to the fractional degree of unfolding, it can be shown that

$$\sigma^{-1/2} = (\langle \Delta C_p \rangle)_{max} \cdot 4RT_m^2 / \Delta h_c^2 \qquad (22)$$

Thus, the three parameters required to define the theoretical statistical mechanical model to this system are obtainable from a single heat-capacity curve. The evaluation of these parameters and the application of the particular theory allow calculation of the overall thermody-

TABLE 2

Thermodynamic Parameters Associated with the Helix-coil Transition of Polypeptides

Polypeptide	ΔH[a]	T_m (°C)	σ[b]	Solvent	Reference
Poly (γ-benzyl L-gluta-mate)	950 ± 20[c]	55	1.28×10^{-4}	85wt% DCA-EDC	14
		42	0.98×10^{-4}	82wt% DCA-EDC	14

[a] cal/mol of amino acid residue.
[b] Cooperativity parameter. See text for details.
[c] Extrapolated value to infinite dilution.
[d] DCA: dichloracetic acid; EDC: 1,2-dichloroethane.

namic functions, including helical distribution functions, for the transition. It has been shown that the assumption of a specific model is not required, however, to obtain this information if the entire C_p curve is used in the analysis.[32] This point will be discussed in a later section.

Ackermann[14] has shown that Δh_c, Δs_c, and σ, as calculated by the above procedure, are dependent upon the polypeptide and upon the exact solvent conditions. A summary of his results is given in Table 2.

Polynucleotides

Complimentary polynucleotides, such as poly (A)· poly (A), poly (A) poly (U), and poly (dAT) · poly (dAT), form well-defined double-stranded and, occasionally, triple-stranded structures in aqueous solution. Disruption of these helical structures occurs upon increasing the temperature, giving rise to anomalous heat- capacity curves such as that shown in Figure 4. The broken line is the excess enthalpy function, $\langle\Delta H\rangle$, calculated by direct integration of $\langle\Delta C_p\rangle \equiv C_p(T) - C_{p,o}(T)$. The area under $\langle\Delta C_p\rangle$ provides an estimate of the enthalpy change for the transition from the double-stranded to the single-stranded form.

The strand-separation reaction occurs abruptly near the maximum in $\langle\Delta C_p\rangle$. The gradual increase in $\langle\Delta C_p\rangle$ prior to strand separation is due to the partial unraveling at the ends of the double strand and the formation of non-base-paired loops within the helical duplex. An apparent ΔC_p between the double- and single-stranded forms is to be noted. This ΔC_p is primarily the result of temperature-dependent changes in the degree of base stacking in the single-stranded forms.[48]

Neumann and Ackermann[16] have calculated

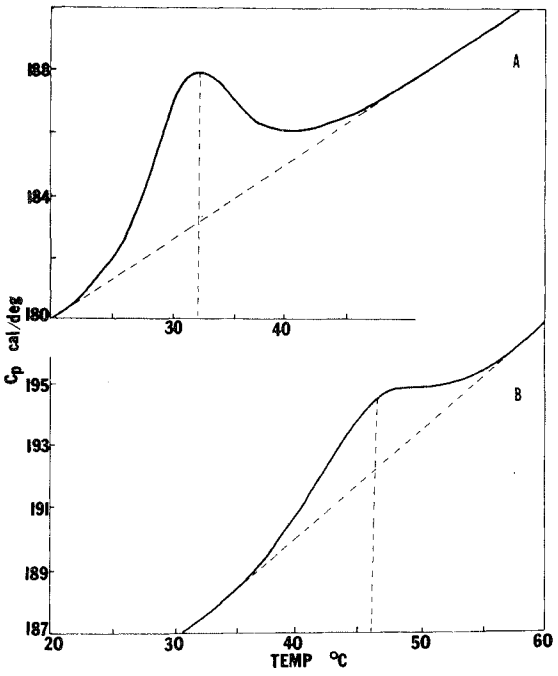

FIGURE 3. Heat capacity as a function of temperature of two poly(γ-benzyl L-glutamate) solutions of equal concentration (0.25 *M*) and of different dichloroacetic acetic acid content (A: 81 wt% DCA; B: 85 wt% DCA). Under these solvent conditions, the transition is from coil to helix upon increasing the temperature. (Adapted from Ackermann, T. and Neumann, E., *Biopolymers*, 5, 649, 1967. With permission.)

cooperative interaction parameters and average helical lengths at the transition temperature using specific theoretical models. These parameters are useful in comparing theoretical results [38,52] with experimental data, but, as with polypeptide systems, such information can be extracted from $\langle\Delta C_p\rangle$ curves without explicit assumptions of a particular model.[40] The

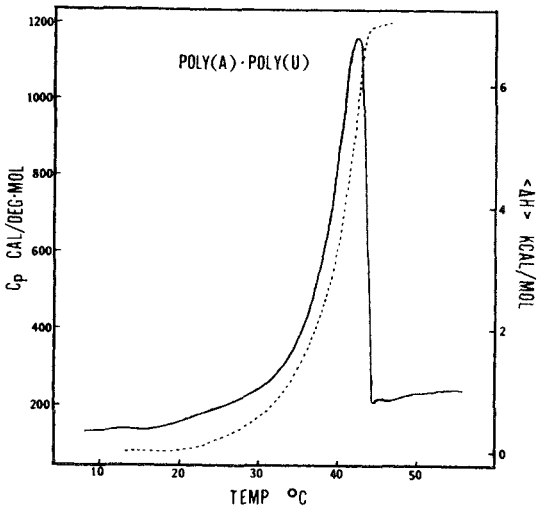

FIGURE 4. C_p vs. temperature (solid line) for the helix-coil transition of poly(A) · poly(U) at neutral pH and [Na^+] = 0.016 *M*. The dashed line (<ΔH>) is the average excess enthalpy calculated by direct integration of C_p after subtraction of $C_{p,o}$. (From Suurkuusk, J., Alvarez, J., Freire, E., and Biltonen, R., *Biopolymers*, 16, 2641, 1977. With permission.)

thermodynamic results for a number of polynucleotide systems are summarized in Table 3.

Proteins

The broadest application of the differential scanning calorimetric technique has been the study of the reversible thermal unfolding of globular proteins in aqueous solution. A typical heat-capacity profile for a globular protein is shown in Figure 5. The salient features are the pronounced temperature dependence of C_p prior to the occurrence of the maximum in C_p and the large difference between C_p before and after the transition. This type of data has been interpreted to indicate a large $\frac{dC_{p,o}}{dT}$ for the folded low-temperature form and a large ΔC_p for the transition.

The temperature dependence of $C_{p,o}$ for the folded state is estimated by the broken line in Figure 5, which upon subtraction yields the excess heat-capacity function, $<\Delta C_p>$. Integration of $<\Delta C_p>$ over the entire transition interval yields a ΔH value which is extremely temperature dependent. This temperature dependence in ΔH, resulting from a nonzero ΔC_p, has been interpreted to be the result of a positive increase in ΔC_p upon unfolding, due to the exposure of previously buried hydrophobic groups to the aqueous medium.[12,53-55]

Lumry et al.[12] have previously shown that the van't Hoff heat for such a transition, ΔH_{vH}, will be less than or equal to the calorimetrically determined enthalpy change:

$$\Delta H_{VH} \leqq \Delta H \qquad (23)$$

TABLE 3

Thermodynamic Parameters Associated with the Double-strand Single-strand Transition of Polynucleotides

System	ΔH[a]	T_m (°C)	ΔC_p[b]	Salt concentration	Reference
Poly(A) · Poly(U)	6.8	42.2	80	0.016 *M* Na^+	48
	7.8	58.2	100	0.16 *M* Na^+	48
	8.6	62.5	95	0.26 *M* Na^+	48
	7.4	44.5	—	0.018 *M* Na^+	49
	7.95	51.3	—	0.043 *M* Na^+	49
	8.2	58.2	—	0.103 *M* Na^+	49
Poly(A) · Poly(A)	7.4	52.5	174	0.1 *M* Acetate, 0.1 *M* NaCl, pH 5.4	48
Poly(dAT) · Poly(dAT)	8.1	39.1	23	0.005 *M* $NaClO_4$, 0.001 *M* Cacodylate-citrate	51

[a] kcal/mol of base pair.
[b] cal/K·mol of base pair.

The equality will hold only in the case of two-state transitions. Assuming a two-state transition, one can calculate ΔH_{vH} from the $<\Delta C_p>$ curve, according to

$$\Delta H_{VH} = [(<\Delta C_p>)_{max}\ 4RT^2]^{1/2} \quad (24)$$

where $(<\Delta C_p>)_{max}$ is the excess heat capacity at the transition temperature. Jackson and Brandts[6] have shown that $\Delta H_{vH} = \Delta H$ for the unfolding of chymotrypsinogen, and Privalov and Khechinashvili[18] have shown that $\Delta H/\Delta H_{vH} = 1.05 \pm 0.03$ for a number of proteins. These results clearly demonstrate that, to a good approximation, the unfolding of many low molecular weight globular proteins is a two-state process.

It is presently clear that globular proteins unfold via approximate two-state processes, that the heat capacity of the folded form is very temperature dependent, and that a substantial increase in C_p occurs upon unfolding. The results of the analysis of several protein systems described above are summarized in Table 4.

Transfer Ribonucleic Acids

The study of the thermal unfolding of transfer ribonucleic acids using differential scanning calorimetric techniques has been rather limited; only four reports currently exist in the literature. Nevertheless, the results of these studies have been of substantial value. Brandts et al.[19] unequivocally demonstrated that since $\Delta H/\Delta H_{vH} >> 1$, the unfolding of tRNA was not a two-state process. Their results also indicated

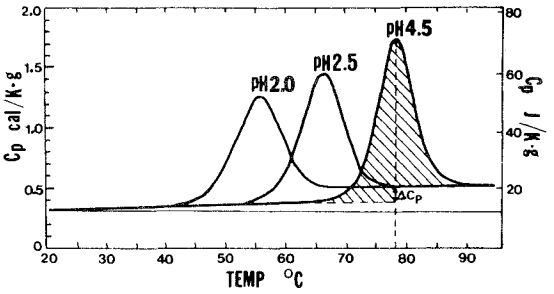

FIGURE 5. Temperature dependence of partial heat capacity of lysozyme at pH values 2.0, 2.5, and 4.5. (From Privalov, P. and Khechinashvili, N., *J. Mol. Biol.*, 86, 665, 1974. With permission.)

that $\Delta H \simeq 200$ kcal/mol and that $\Delta C_p = 1$ to 7 kcal/K·mol. These values are much larger than those found for proteins of the same molecular weight.

Privalov and co-workers[20,21] arrived at similar conclusions, except that they asserted that C_p of the folded state is very temperature dependent and that ΔC_p is not particularly large. They suggested that the large ΔC_p values which were obtained in the presence of Mg^{2+}, under which conditions tRNA tends to be hydrolyzed, were the result of the transition not being reversible.

A typical $<\Delta C_p>$ profile for tRNA is shown in Figure 6. The salient feature of this transition is that it occurs over a very broad temperature range. Privalov and co-workers[20,21] have attempted to define this complex transition in terms of a number of independent two-state

TABLE 4

Thermodynamic Parameters Associated with the Thermal Unfolding of Globular Proteins

Protein	ΔH (kcal/mol)	T_m (°C)	ΔC_p (kcal/K·mol)	Solvent	Reference
Ribonuclease	88	40.6	2.1	0.2 *M* Glycine, pH 2.8	47
	90[a]	43.0[a]	1.3[a]	0.04 *M* Glycine, pH 2.8	18
	95 ± 5	43.0	1.8 ± 0.5	0.2 *M* Glycine, pH 2.8	27
Chymotrypsinogen	102	42.0	3.3	HCl, pH 2.03	6
	135	54.2	2.8	0.05 *M* Glycine, pH 3.02	6
α-Chymotrypsin	95[a]	44.0[a]	3.2	0.04 *M* Glycine, pH 2.6	18
Lysozyme	90[a]	53.0[a]	1.6[a]	0.04 *M* Glycine, pH 2	18
Cytochrome c	70[a]	59.0[a]	1.7[a]	0.04 *M* Glycine, pH 3	18

[a] Values estimated from figures in the original reference.

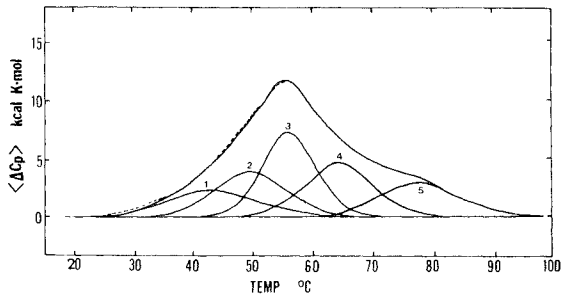

FIGURE 6. Decomposition of the excess heat capacity function of $tRNA^{Phe}$ (yeast) in terms of five independent two-state transitions. Dotted line: experimental curve; solid line: summation of the functions 1 to 5. Solvent: 5 m*M* sodium phosphate, 1 m*M* EDTA, 150 m*M* NaCl, pH 7.0. (From Hinz, H., Filiminov, V., and Privalov, P., *Eur. J. Biochem.*, 72, 79, 1977. With permission.)

transitions, as depicted by the solid lines in Figure 6. In such a case and assuming $\Delta C_{p,i} = 0$,

$$<\Delta C_p> = \sum_i \frac{K_i}{(1 + K_i)^2} \frac{\Delta H_i^2}{4RT^2} \quad (25)$$

where K_i and ΔH_i are the equilibrium constants and enthalpy changes of the independent transitions. The results of one such analysis are tabulated in Table 5.

The type of analysis suggested by Privalov and co-workers[20,21] is correct in special cases but is not valid for all situations. In any case, it is now clear that the thermal transitions of tRNA are multistate and exhibit enthalpy changes of about 300 kcal/mol for the overall transition. In subsequent sections of this review, appropriate procedures for obtaining a detailed description of their thermal behavior will be discussed.

Gel-liquid Crystalline Transition in Phospholipid Bilayers

Pure phosphatidylcholine and other phospholipids can form either single lamellar or multilamellar vesicles in an aqueous dispersion.[22] These dispersions undergo thermally induced transitions in state which can be monitored with a differential scanning calorimeter.[11,23-25] A typical C_p curve for multilamellar dipalmitoylphosphatidylcholine (DPPC) liposomes is shown in Figure 7. Two transitions are observed. The first at about 35°C presumably involves reorientation of the charged head groups. However, this change in state is slow, and the apparent C_p function does not represent an equilibrium situation.[11,56,57] The second transition at 41°C is rapid, and the C_p function in this region represents a change from a state in which the aliphatic side chains are relatively rigid and in close van der Waal's contact with its neighbors to a state in which essentially free rotation about the carbon-carbon bonds is allowed.

This main transition, with an associated $\Delta H = 8.7$ kcal/mol, is definitely not a two-state transition. The typical information derived from this transition curve includes ΔH, the melting temperature, T_m, and an apparent cooperative unit calculated from

$$n = \frac{(<\Delta C_p>)_{max} \cdot 4RT_m^2}{\Delta H^2} \quad (26)$$

It has been found that changes in the average size of the vesicle, the size of the phospholipid, and the presence of small molecules such as anesthetics and cholesterol alter the characteristics of the main transition. The results obtained for several such systems are summarized in Table 6.

Although no attempt at a detailed analysis of the statistical thermodynamic description of the gel-liquid crystalline transition of phospholipids has been published, the basic analytical protocol to do so will be described in the following section. It will be demonstrated that the distribution of cluster sizes and changes therein can be obtained from appropriate analysis of the C_p data.

A GENERAL STATISTICAL THERMODYNAMIC DESCRIPTION

In the preceding section, the results of the analysis of C_p for several different systems were presented. For the most part, these analyses have focused upon the evaluation of ΔH for the transition and, in a few cases, evaluation of certain model-based quantities. The most significant conclusion of these studies has been the validation of the two-state approximation for proteins. Except in the case of the analysis of tRNA data, the detailed shape of the C_p curve has been ignored. In the following discussion, procedures proposed by Freire and

TABLE 5

Thermodynamic Parameters from Decomposition of $tRNA^{Phe}$ (Yeast) Heat-capacity Curves Assuming a Model of Independent Transitions

Solvent	ΔH_1 (kcal/mol)	$T_{m,1}$ (°C)	ΔH_2 (kcal/mol)	$T_{m,2}$ (°C)	ΔH_3 (kcal/mol)	$T_{m,3}$ (°C)	ΔH_4 (kcal/mol)	$T_{m,4}$ (°C)	ΔH_5 (kcal/mol)	$T_{m,5}$ (°C)
10 m*M* Sodium cacodylate, 20 m*M* NaCl, 1 m*M* EDTA, pH 6.8	45	26	52	41.3	76	41	69	50.5	57	62
5 m*M* Sodium phosphate, 150 m*M* NaCl, 1 m*M* EDTA, pH 7.0	45	43	60	50	82	56.3	68	65	58	78

Taken from Hinz, H., Filiminov, V., and Privalov, P., *Eur. J. Biochem.*, 72, 79, 1977. With permission.

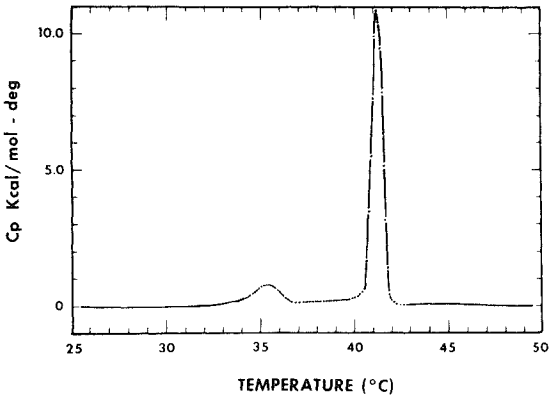

FIGURE 7. Excess heat capacity function of a fresh dispersion of multilamellar liposomes prepared from DPPC in 0.05 *M* KCl. (Reprinted with permission from Suurkuusk, J., Lentz, B., Barenholz, Y., Biltonen, R., and Thompson, T., *Biochemistry*, 15, 1393, 1976. Copyright by the American Chemical Society.)

Biltonen[27,32,40] by which statistical thermodynamic descriptions of thermally induced processes of macromolecular systems can be obtained from C_p data will be reviewed. Let us begin by considering the general statistical thermodynamic properties of such systems.

The Configurational Partition Function

From the point of view of statistical thermodynamics, definition of a function, $\mathcal{Z}$ called the "configurational" or "molecular partition function," is sufficient to specify the system in terms of molecular distributions and its average thermodynamic properties. This function is obtained by summing the statistical weights, W_c of all accessible configurations or conformational states of the molecule,

$$\mathcal{Z} = \sum_c W_c \tag{27}$$

The statistical weight, W_c, is the absolute probability of the macromolecule existing in the conformational state, c, which can be expressed in terms of the Maxwell-Boltzmann term, $e^{-G_c/RT}$, where G_c is the Gibbs energy of the conformation c, R the universal gas constant, and T the absolute temperature. It follows that conformations with the same Gibbs energy have exactly the same probability of occurrence.

The sum over conformations included in the partition function can be transformed into a sum over energies by grouping together all conformations sharing the same Gibbs energy, G_i,

$$\mathcal{Z} = \sum_i^n \omega_i e^{-G_i/RT} \tag{28}$$

where ω_i is the number of distinct states of energy G_i.

In the study of conformational transitions, relative energy changes are of more interest

TABLE 6

Thermodynamic Parameters Associated with the Gel-liquid Crystalline Transition of Multilamellar Phospholipid Vesicles

	Pretransition			Main transition			
Phospholipid	ΔH[a]	T_m[b] (°C)	n[c]	ΔH[a]	T_m[b] (°C)	n[c]	Reference
DPPC	2.3	34.0	70	9.69	41.75	70	23
DPPC	1.6	35.4		8.2	41.2		11
DPPC	1.8	35.3	290	8.7	41.4	260	24
DMPC[d]	1.1	13.5	200	6.26	23.7	200	23
DMPC	1.0	14.2	280	5.4	23.9	330	24
DSPC[e]	1.4	49.1	230	10.84	58.24	80	23
DSPC	1.8	51.5	160	10.6	54.9	130	24
DLPC[f]				1.7	−1.8	980	24

[a] kcal/mol of phospholipid molecule.
[b] Temperature of the maximum in Cp.
[c] Cooperative unit (molecules).
[d] Dimyristoylphosphatidylcholine.
[e] Distearoylphosphatidylcholine.
[f] Dilauroylphosphatidylcholine.

than absolute energy values. Therefore, it is important to introduce reference states to which the thermodynamic quantities associated with the transitions can be referred. It is convenient to use some well-defined macromolecular states such as the folded (native) state or the completely unfolded state of the molecule as a reference state. Hence, we will introduce the "partition functions" Q and Z, defined as follows: Q is the ratio between $\mathcal{Z}$ and the statistical weight of the state of lowest enthalpy; Z is the ratio between $\mathcal{Z}$ and the statistical weight of the final or highest enthalpy state. Thus, Z and Q differ only in the choice of the reference state; therefore,

$$\frac{Q}{Z} = e^{-\Delta G/RT} \tag{29}$$

where $\Delta G = G_n - G_o$ is the Gibbs energy difference between the final, high-temperature state and the low-temperature state. It will be shown later that Q and Z contain all the information required for a complete thermodynamic description of the conformational equilibria of a homogeneous system and, furthermore, that both quantities can be experimentally evaluated from the heat-capacity function.

Macroscopic Averages and the Partition Function

Consider a solution of N_T molecules (N_T being of the order of Avogadro's number, though not necessarily identical). Let y_k be the mole fraction of molecules of type k

$$y_k = \frac{\#_k}{N_T} \tag{30}$$

$$\Sigma y_k = 1 \tag{30a}$$

where $\#_k$ is the total number of molecules of type k in the solution. Assume that the solution is sufficiently dilute so that the molecules do not interact with one another. Let X be any property of the system dependent upon its energy. The average value of X, $\overline{X}$, is an average over all the species in solution and can be represented as

$$\overline{X} = \sum_k y_k \langle X_k \rangle \tag{31}$$

where $\langle X_k \rangle$ is the average value of X per mole of species k. In this notation, $\overline{X}$ is an average over different species, while $\langle X_k \rangle$ is an average over all configurations of the same species;

$$\langle X_k \rangle = \Sigma F_{k,i} X_{k,i} \tag{32}$$

where $F_{k,i}$ is the relative fraction of molecules of type k populating the i^{th} Gibbs energy state accessible to this species. The distribution of molecules of the same species among its accessible energy states is a Maxwell-Boltzmann distribution, so that $F_{k,i}$ can be written as

$$F_{k,i} = \frac{\omega_{k,i} e^{-G_{k,i}/RT}}{\sum_i \omega_{k,i} e^{-G_{k,i}/RT}} \tag{33}$$

where $\omega_{k,i}$ is the degeneracy of the i^{th} energy state accessible to species k. In terms of the partition function Q_k, $F_{k,i}$ is written as

$$F_{k,i} = \frac{\omega_{k,i} e^{-\Delta G_{k,i}/RT}}{Q_k} \tag{34}$$

where $\Delta G_{k,i} = (G_{k,i} - G_{k,o})$. The average excess enthalpy $\langle \Delta H_k \rangle$ is defined as in Equation 32 and, by virtue of Equations 33 and 34, is equal to

$$\langle \Delta H_k \rangle = RT^2 \frac{\partial \ln Q_k}{\partial T} \tag{35}$$

The average excess enthalpy of the whole system, $\overline{\Delta H}$, is then

$$\overline{\Delta H} = \Sigma y_k \langle \Delta H_k \rangle = RT^2 \Sigma y_k \frac{\partial \ln Q_k}{\partial T}$$

$$= RT^2 \frac{\partial}{\partial T} \Sigma y_k \ln Q_k \tag{36}$$

Equation 36 is the fundamental linkage relation between experimental thermodynamic quantities and the microscopic molecular parameters contained in the partition function of the system.

Integral Representation of the Partition Function

Equation 36 can be rewritten in an integral form as

$$\Psi = \Sigma y_k \ln Q_k = \int_{T_o}^{T} \frac{\overline{\Delta H}}{RT^2} dT \tag{37}$$

and numerically solved for ψ at any tempera-

ture, T, if ΔH is known as a function of temperature. T_o is defined as the temperature at which all the molecules exist in their lowest energy state.

Freire[26] has demonstrated that the integrand of Equation 37 satisfies a Lipschitz condition with reference to ψ, so that Equation 36 has one and only one solution. In addition, the integral solution is numerically stable with respect to the initial conditions, i.e., if the initial conditions at T_o are altered by a very small amount, then the solution is altered very little for all $T > T_o$.

Equation 37 is an integral representation of the logarithm of the partition function of the internal degrees of freedom of the molecules in solution. As a partition function, e^{ψ} is constructed from contributions of all the conformational states of all the molecules in solution. However, since all the quantities have been defined in terms of thermodynamic excess functions, e^{ψ} is not exactly the partition function of the solution as a whole but only of the conformational properties of the molecules in solution. In studying conformational transitions in macromolecules, this is precisely the quantity of interest.

In the derivation of Equation 37, no explicit reference to the nature of y_k was made. Actually, y_k, as a distribution function, is arbitrary and may or may not follow any specified law. Since y_k measures the relative population of species k in the solution, it will always depend on the particular conditions of the experiment. Accordingly, the simplest case is that of a homogeneous, one-component system in which the solution is composed of a single macromolecular species; in this instance, $y_k = 1$, $\Delta H = \langle \Delta H \rangle$, and e^{ψ} is equal to the partition function, Q.

Equation 37 thus offers the unique opportunity of evaluating the partition function of a system from the average excess enthalpy function which is obtainable from calorimetric data. It should be emphasized that the derivation of Equation 37 involved only thermodynamic considerations. Therefore, its solution is general and independent of any particular model or mechanism of the transition. Furthermore, it is also valid for a heterogeneous multicomponent system. This is an advantage if one considers that only a few simple systems have a mathematically analytical partition function. Having numerically defined the partition function, one can calculate the molecular averages and molecular distribution functions, as will be discussed in the next sections.

MULTISTATE TRANSITIONS

A considerable body of calorimetric data has shown that the thermal unfolding of globular proteins is well approximated as a two-state process. This fact allows one to obtain reliable thermodynamic information for these conformational transitions by monitoring the temperature-induced change of any appropriate observable. Such is not the case for fibrous proteins, nucleic acids, synthetic polypeptides, synthetic polynucleotides, and biomembranes. In such systems, deviations from the two-state process are of such magnitude that thermodynamic information is not directly available from a single melting profile.

Multistate transitions have usually been analyzed by comparison of the experimental melting profile to one derived from a theoretical model for the reaction. In doing this, several approximations for the partition function have been developed, and the thermodynamic information has been indirectly obtained by fitting the experimental data to theoretical equations derived from the model. For this reason, reliable thermodynamic information has generally been restricted to molecules in which the contribution of each residue to the actual value of the observable is known or can be assumed to be the same for each. For a multistate transition, melting profiles obtained with different physical observables are not necessarily identical. Recently, Freire and Biltonen[27] demonstrated that all relevant thermodynamic information for a sequential multistate transition can be obtained by proper analysis of the excess heat-capacity function of the system. Their development will be reviewed here.

A generalized multistate transition is described by Equation 1 in terms of a sequential mechanism in which a macromolecule in its folded state (I_o) undergoes a melting transition to an unfolded state (I_n) through (n−1) intermediate states. The partition function of such systems (Equation 3) can be written as

$$Q = 1 + \sum_{i-1}^{n} e^{-\Delta G_i/RT} \quad (38)$$

where the initial state is taken as the reference state; and $\Delta G_i = G_i - G_o$ is the Gibbs energy difference between the i^{th} and the reference state. The fraction of molecules in the i^{th} state, F_i, defined as the ratio of the concentration of molecules in the i^{th} state to the total concentration, is

$$F_i = \frac{[I_i]}{\sum_{i=1}^{n} [I_i]} = \frac{e^{-\Delta G_i/RT}}{Q} \quad (39)$$

The identity $\sum_{i=0}^{n} F_i = 1$ is satisfied at all temperatures. And $<\Delta H>$ is given by

$$<\Delta H> = \sum_{i=0}^{n} \Delta H_i F_i \quad (40)$$

where ΔH_i is the enthalpy difference at any temperature between the i^{th} state and the reference state, i.e., $\Delta H_i = (H_i - H_o)$. Each F_i term can be written in terms of the partition function, Q, of the system, such that Equation 40 becomes

$$<\Delta H> = \frac{\sum_{j=0}^{n} \Delta H_i e^{-\Delta G_i/RT}}{Q} \quad (41)$$

The fact that ΔH_i occurs both as a coefficient and in the exponential of each term in Equation 41 is a unique feature of the enthalpy and is not satisfied by any other physical observable other than the volume change. The characteristic values, α_i, of any other physical observable are not correlated with their respective exponents; therefore, it is impossible to obtain direct thermodynamic information from the melting profile of a multistate transition. This is not the case when $<\Delta H>$ is the observable. Equation 41 written in differential form as

$$d(\ln Q) = \frac{<\Delta H>}{RT^2} dT \quad (42)$$

can numerically be evaluated to yield the partition function, Q. Having the partition function, one can obtain the thermodynamics of the system.

$<\Delta H>$ can be evaluated as a continuous function of the temperature by integration of the excess apparent molar heat capacity of the system, $<\Delta C_p>$, estimated from differential scanning calorimetric data. The quantity measured by the calorimeter is the apparent molar heat capacity which at any temperature, T, is related to $<\Delta H>$ by the integral relation

$$<\Delta H> = \int_{T_o}^{T} (C_p - C_{p,o})\, dT$$

where $C_{p,o}$ is the apparent molar heat capacity of the initial state.

Integration of Equation 42 yields

$$\ln Q = \int_{T_o}^{T} \frac{<\Delta H>}{RT^2} dT \quad (44)$$

where T_o is a temperature at which all molecules exist in the initial state. In a rigorous sense, T_o should be absolute zero since no finite temperature exists in which a single state can account for 100% of the population. However, it has been shown that negligible error is introduced by using as T_o the smallest finite temperature at which a physically detectable change in the system can be observed.

It is to be noted that the reference state does not contribute to $<\Delta H>$ and that the other states make significant contributions to $<\Delta H>$ only when they become populated. Therefore, Q is a relatively insensitive function of temperature at temperatures below the transition temperature.

Equation 44 allows calculation of the partition function of the system from the average excess enthalpy function. The fraction of molecules in the initial state can then be calculated by noting that

$$F_o = \frac{1}{Q} = \exp\left(-\int_{T_o}^{T} \frac{<\Delta H>}{RT^2} dT\right) \quad (45)$$

The fraction of molecules in the final unfolded state (F_n) can also be calculated by noting that

$$\frac{dF_n}{dT} = \frac{F_n}{RT^2} (\Delta H_n - <\Delta H>) \quad (46)$$

from which

$$F_n = \frac{1}{Z} = \exp\left(-\int_{T}^{T_n} (\Delta H_n - \langle \Delta H \rangle) \frac{1}{RT^2}\, dT\right) \quad (47)$$

can be evaluated. T_n is defined in analogous form to T_o (all molecules exist in the final state at T_n), and ΔH_n is the enthalpy change associated with the complete transition, $I_o \rightarrow I_n$.

The fraction of molecules populating all intermediate states, F_I, is

$$F_I = 1 - F_o - F_n \quad (48)$$

For a transition of the two-state type, F_I, is identically zero at all temperatures, and F_n, defined by Equation 47, is equal to the apparent fraction of unfolded molecules, F_{app}, defined in the conventional form as the fractional degree of change of the observable with which the transition is being measured. Equation 48 allows not only testing of the two-state hypothesis but quantitative estimation of the overall population of intermediate states existing during the transition. A further test can be performed by noting that the quantity, $\langle \Delta H \rangle/(1 - F_o)$, defined as

$$\frac{\langle \Delta H \rangle}{1 - F_o} = \frac{\sum_{i=1}^{n} \Delta H_i e^{-\Delta G_i/RT}}{\sum_{i=1}^{n} e^{-\Delta G_i/RT}} \quad (49)$$

is, at all temperatures, identically equal to the total enthalpy change for the transition if and only if the transition is of the two-state type. As we shall see later, Equation 49 also provides the basis for the entire deconvolution of the melting profile of a multistate transition into population fractions.

DECONVOLUTION ANALYSIS OF THE THERMAL UNFOLDING OF RIBONUCLEASE A

Freire and Biltonen[27] have applied this analysis to test the two-state hypothesis for the thermal unfolding of ribonuclease A, as described below. In Figure 8, the apparent molar heat-capacity function (C_p) and the average excess enthalpy ($\langle \Delta H \rangle$) of ribonuclease A at pH 2.8 are shown. Under the conditions of this experiment, ribonuclease A undergoes a reversible thermal unfolding characterized by the thermodynamic parameters previously summarized in Table 4. $\langle \Delta H \rangle$ was calculated according to Equation 43, assuming that $C_{p,o}$ is given by the linear extrapolation of the low-temperature C_p curve. $\Delta h_i = \langle \Delta H \rangle/(1-F_o)$ is shown as the broken line in Figure 8. The nonconstant value of Δh_i is consistent with an average $\Delta C_p^\circ = 2$ kcal/mol for the transition over the given temperature interval.

The results of the deconvolution analysis of this experiment are presented in Figure 9. In this figure, the fraction of molecules populating the initial and final states is plotted as a function of temperature; F_o and F_n were calculated with Equations 45 and 47, respectively. The fraction of molecules populating intermediate

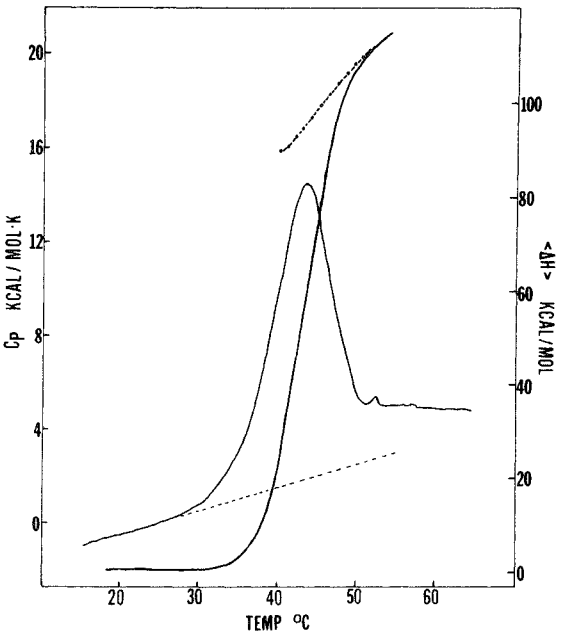

FIGURE 8. Experimental C_p and $\langle \Delta H \rangle$ vs. temperature profiles of Ribonuclease A. The upper dotted line is the experimental $\langle \Delta H \rangle/(1 - F_o)$ function which for a two-state transition is equal to the overall enthalpy change for the transition. The nonconstant value for ΔH reflects the difference in C_p between the initial and final states. $C_{p,o}$ (bottom dotted line) was calculated by a least-squares fit of the heat capacity function up to 25°C. The experimental conditions were as follows: 0.2 *M* glycine buffer, 1 m*M* EDTA at pH 2.8, 9 mg/ml RNAse concentration in the calorimetric cell. (From Freire, E. and Biltonen, R., *Biopolymers*, 17, 463, 1978. With permission.)

states ($F_i = 1 - F_o - F_n$) is also shown. At no temperature is the fraction of intermediates greater than 5% of the total population, i.e., the fraction of molecules in the initial and final states always accounts for at least 95% of the total population. This conclusion supports the two-state model as a first approximation to this transition.

This procedure for testing the two-state hypothesis for a thermal transition should be more sensitive than a simple comparison of the integrated enthalpy change with the van't Hoff heat obtained from a slope at the T_m. The small deviation from exact two-state behavior appears to be real and agrees with Privalov's observation[18] of an average $\Delta H/\Delta H_{vH}$ ratio of 1.05 for several proteins. Thus, this apparent deviation from two-state behavior is probably not an experimental or analytical artifact but a characteristic of the transition.

DECONVOLUTION OF A MULTISTATE TRANSITION

For a multistate transition, the quantity $\langle\Delta H\rangle/(1-F_o)$, defined by Equation 49, is an S-shaped curve whose lower limit is equal to the enthalpy difference, Δh_1, between the first intermediate and the initial state. In this case, Equation 49 can be rewritten as

$$\frac{\langle\Delta H\rangle}{1 - F_o} = \Delta h_1 + \frac{\Sigma\, \Delta H_i e^{-\Delta G_i/RT}}{Q_1} \qquad (50)$$

$$= \Delta h_1 + \langle \Delta H_1 \rangle \qquad (50a)$$

The function $\langle\Delta H_1\rangle$ defines a new average excess enthalpy, but one which is averaged over all energy states except the first. Similarly, Q_1 as a partition function is obtained by summing the statistical weights of all energy states except the first. Q_1 and $\langle H_1\rangle$ are related by the integral equation

$$Q_1 = \exp\left(\int_{T_o}^{T} \frac{\langle\Delta H_1\rangle}{RT^2}\, dT\right) \qquad (51)$$

and can be experimentally obtained after evaluation of Δh_1, as previously described. Q_1 can then be used to define a subfraction ($F'_1 = Q^{-1}{}_1$) of molecules in the first intermediate state. It must be noted that F'_1 is not an average over all the accessible energy states of the system but only over those states included in Q_1.

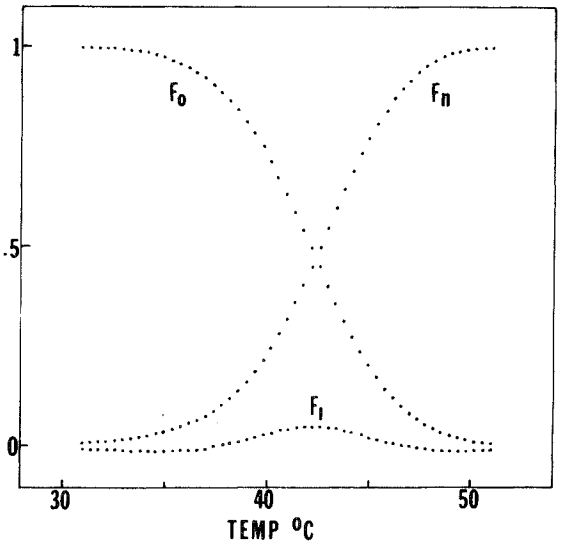

FIGURE 9. The experimentally calculated relative population of states associated with the thermal unfolding of Ribonuclease A. F_o and F_n are the fraction of molecules populating the initial and final states, respectively. F_I is the summed population of all intermediates. This result clearly demonstrates that this transition is well approximated as a two-state transition; at no temperature is F_I greater than 5% of the total population. (From Freire, E. and Biltonen, R., *Biopolymers*, in press. With permission.)

The above mathematical procedure is equivalent to eliminating the contributions of the initial state to the thermodynamic parameters describing the transition. From a mathematical standpoint, we have reduced the number of energy states by one, and all remaining functions are analogous to those that one would find if the first intermediate state were the lowest enthalpy state and the initial state did not exist.

This procedure can be successively repeated to yield a set of recursion relations[27] from which all the $\Delta h_i \equiv \Delta H_i - \Delta H_{i-1}$, F_i', and Q_i can be estimated. In general,

$$\langle\Delta H_{i+1}\rangle = \frac{\langle\Delta H_i\rangle}{1 - F_i'} - \Delta h_{i+1} \qquad (52)$$

$$F_i' = Q_i^{-1} = \exp\left(-\int_{T_o}^{T} \frac{\langle\Delta H_i\rangle}{RT^2}\, dT\right) \qquad (53)$$

from which all the thermodynamic parameters describing each transition of the unfolding reaction can be evaluated. In particular, each $T_{m,i}$ is equal to the temperature at which $F_{i-1} = F_i$,

TABLE 7

Thermodynamic Parameters Associated with the Melting Transition of Figure 10

$$I_0 \overset{K_1}{\longleftrightarrow} I_1 \overset{K_2}{\longleftrightarrow} I_2 \overset{K_3}{\longleftrightarrow} I_3 \overset{K_4}{\longleftrightarrow} I_4$$

Transition	Δh_i[a] (kcal/mol)	Δh_i[b] (kcal/mol)	$T_{m,i}$[c] (°C)	$T_{m,i}$[d] (°C)
1	60	60.7	30	29.89
2	60	60.01	40	39.97
3	100	101.2	50	49.99
4	100	99.6	60	59.99

[a] Actual value.
[b] Obtained from deconvolution analysis.
[c] Actual value.
[d] Obtained from deconvolution analysis.

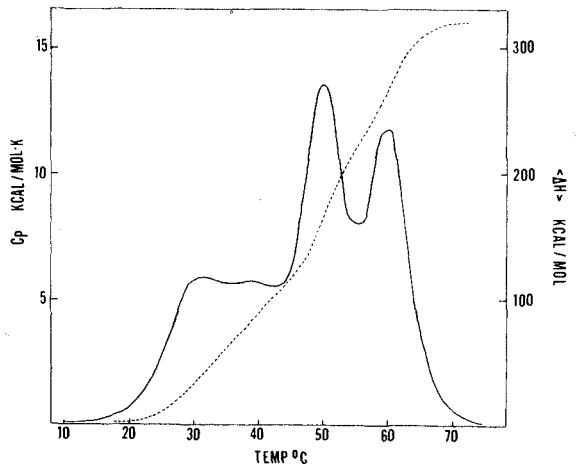

FIGURE 10. Computer-simulated C_p (—) and $\langle\Delta H\rangle$ (———) vs. temperature for the multistate transition described in Table 7. (From Freire, E. and Biltonen, R., *Biopolymers*, 17, 463, 1968.

so that $\Delta s_i = \Delta h_i/T_{m,i}$. Each of the equilibrium constants, K_i, defined in Equation 5 can be calculated by

$$K_i = \exp\left(-\frac{\Delta h_i}{RT} + \frac{\Delta s_i}{R}\right) \tag{54}$$

or by use of the relation:

$$K_i = \frac{Q_{i-1}^{-1}}{Q_i} \tag{55}$$

Absolute fractions of molecules in each particular state i, defined by Equation 39, can be expressed in a recursive form as

$$F_i = F_{i-1} K_i$$

$$= F_{i-1} \frac{(Q_{i-1} - 1)}{Q_i} \tag{56}$$

from which the relative population of each state as a continuous function of the temperature is obtained.

GENERAL APPLICATION TO MULTISTATE TRANSITIONS

In principle, the deconvolution analysis described makes possible the dissection of the melting profile of a multistate transition without any a priori assumptions relating to the thermodynamic mechanism of the reaction. This capability of the method has been demonstrated by Freire and Biltonen,[27] who first applied the procedure to a hypothetical multistate transition whose thermodynamic parameters are summarized in Table 7. In Figure 10, the computer-simulated apparent molar heat-capacity function ($\langle\Delta C_p\rangle$) and the average excess enthalpy ($\langle\Delta H\rangle$) associated with this complex transition have been plotted as a function of the temperature.

Having $\langle\Delta C_p\rangle$ and $\langle\Delta H\rangle$, the typical sequence of calculations in the deconvolution analysis is as follows. First, the partition function of the system, Q, is calculated by numerical integration of Equation 44. Δh_1 is estimated by determining the lower limit of $\langle\Delta H\rangle/(1-F_o)$. By subtraction of Δh_1, $\langle\Delta H\rangle/(1-F_o)$ is then transformed into the excess function $\langle\Delta H_1\rangle$ from which Q_1 is obtained in an analogous way to Q. Successive applications of recursion relations given in Equations 52 and 53 allow calculation of the various Δh_i, Q_i, and $\langle H_i\rangle$ from which the complete set of thermodynamic parameters describing the transition is obtained. This procedure is graphically illustrated in Figure 11, in which the various $\langle H_i\rangle$ have been plotted on the temperature scale.

The accuracy of the method was found to be very high; all the thermodynamic parameters were reproduced with a relative error smaller than 1%. Figure 12 shows the relative population of each state as a function of the temperature; the deviation from the theoretical curves is negligible over the entire temperature range.

The resolving potential of the method was

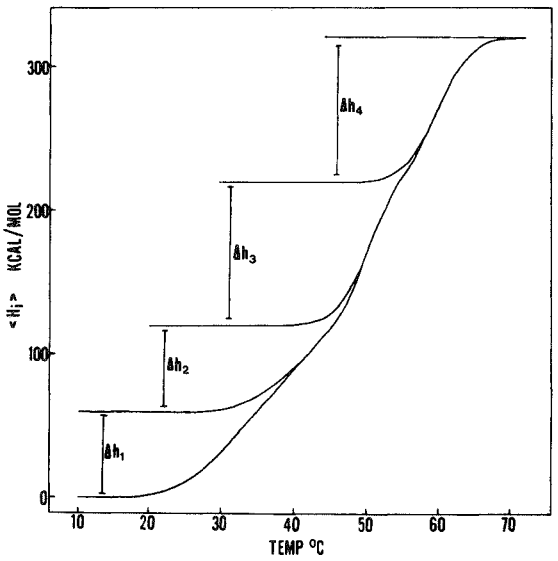

FIGURE 11. Graphic illustration of deconvolution of the multistate transition of Figure 10. The $\langle H_i \rangle$ functions were calculated as described in the text. (From Freire, E. and Biltonen, R., *Biopolymers,* 17, 463, 1978. With permission.)

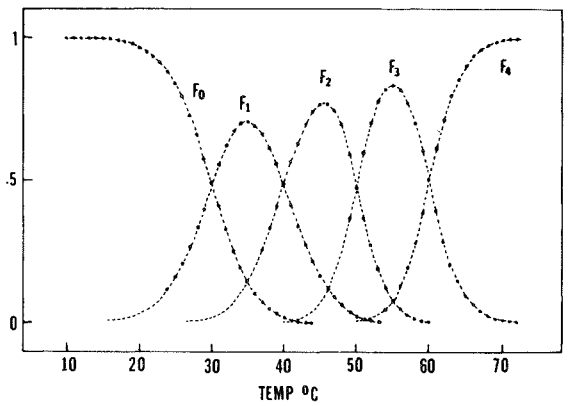

FIGURE 12. Relative population vs. temperature of the five thermodynamic states associated with the multistate transition described in Table 7. (———), theoretical populations; (· · · ·), as obtained from the deconvolution analysis. (From Freire, E. and Biltonen, R., *Biopolymers,* 17, 463, 1978. With permission.)

also examined by decreasing the temperature spacing between the hypothetical transitions. When the temperature spacing between transitions was reduced to 3°C, the heat-capacity curve did not reveal any detail of the nature of the transition or the number of states present. Deconvolution analysis, however, not only identified the number of intermediate states but allowed determination of the thermodynamic parameters for the entire transition with a high degree of accuracy. The comparison between the results of the analysis and the hypothetic parameters is given in Table 7. Computer simulations have also shown that the deconvolution analysis is capable of accurately determining the thermodynamic parameters associated with two transitions having exactly the same melting temperature.

Freire and Biltonen[27] also investigated sources of various errors in this deconvolution analysis. They found that selection of T_o, the initial temperature at which integration is initiated, was not critical. They also discovered that random experimental noise has negligible influence on the results of the analysis, presumably because of the double integration procedure. The major sources of uncertainty were found to be propagation of error due to incorrect estimation of the heat capacity of the reference state and a systematic error due to mistakes in the determination of the concentration of the macromolecule in solution. The former type of error produces a distortion in the $\langle \Delta C_p \rangle$ curve, and the latter type produces a constant percentage error in its magnitude. The effect of these errors is best demonstrated with actual experimental data, as will be given for tRNA in the next section.

THE THERMAL UNFOLDING OF TRANSFER RIBONUCLEIC ACIDS

Brandts,[19] Privalov et al.,[20] Hinz et al.,[21] and Ackermann and co-workers[28] have previously demonstrated that the thermally induced unfolding of tRNA is not a simple two-state process but rather a sequence of transitions. Privalov and co-workers[20,21] have attempted to resolve the overall transition into a sum of independent two-state processes, as discussed in the section on previous calorimetric studies. In certain cases, this procedure will produce a correct description of the system, but, in general, it is inadequate. In this section, the application of the deconvolution procedure to the analysis of the unfolding of tRNA will be described.

The apparent heat-capacity function, C_p, of a tRNA sample containing 0.52 *M* Na^+ and no Mg^{2+} is shown in Figure 13. It is characterized by a melting temperature, T_m, (defined as the position of the maximum in C_p) of 63.4°C and a calorimetric ΔH (the area under the heat-ca-

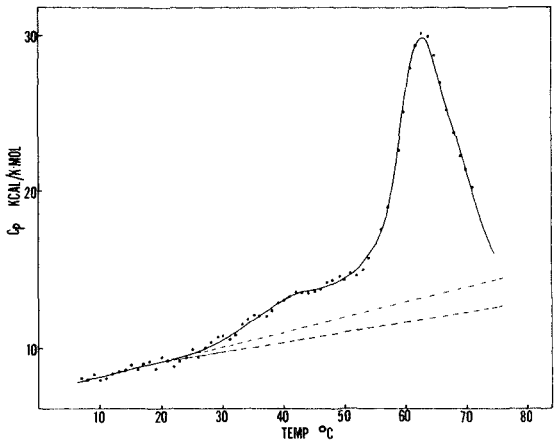

FIGURE 13. C_p vs. temperature profile of $tRNA^{Phe}$ (yeast) at 0.52 M Na^+, (10^{-2} M Na_2HPO_4 — NaH_2PO_4; 0.5 M NaCl; pH 7). The solid line is the simulated C_p profile using the deconvolution parameters (Table 8). The experimental points have been plotted every 1°C; the actual number of points is ten times greater. The dotted lines are the upper and lower baselines considered in the error analysis. (From Freire, E. and Biltonen, R., *Biopolymers*, 17, 1257, 1978. With permission.)

pacity curve in the temperature interval 8 to 72°C) of 260 kcal/mol. The area under the C_p curve was calculated by numerical integration of the quantity ($C_p - C_{p,o}$) where $C_{p,o}$, the heat capacity of the initial state, was assumed to be of the form $C_{p,o} = a + bT$. $C_{p,o}$ was calculated by a linear least-squares fit of the initial part of the scan (8 to 20°C) and then extrapolated forward over the entire transition interval, as shown.

The total enthalpy change for the melting of $tRNA^{Phe}$ under these conditions is of the same magnitude, although somewhat smaller, than that previously reported by Hinz et al.[21] This difference can be accounted for by the heat effect associated with a transition in the high-temperature region (72 to 100°C). Freire and Biltonen have not been able to experimentally define C_p in the high-temperature region, due to technical reasons. (The temperature range of these authors' instrument is 0 to 75°C.) This fact does not affect the deconvolution analysis of the transition in the experimentally accessible temperature. Since the quantity of interest is the excess heat-capacity function ($<\Delta C_p>$) and its calculation is independent of the heat capacity of the final state, the analysis can always be done in the temperature range covered by the experimental data. The deconvolution analysis can be performed even if the transition end point is unknown or experimentally inaccessible.

The average excess enthalpy function, $<\Delta H>$, was calculated by numerical integration of ($<\Delta C_p>$). The partition function, Q, was calculated according to Equation 49. The thermodynamic parameters characterizing the transition were obtained in a recursive form after successive applications of Equations 52 and 53. Each Δh_i was set equal to the limiting value of the function $<\Delta H_{i-1}>/(1 - Q^{-1}_{i-1})$.

In all the calculations, the various Δh_i were assumed to be temperature independent, since Privalov et al. [20] and Hinz et al.[21] have demonstrated that, in the absence of Mg^{2+}, the overall ΔC_p for the transition is not greater than 1 kcal/K·mol, i.e., ~200 cal/K·mol per transition step, a figure lower than the experimental error in determining each Δh_i.

The results of the deconvolution analysis for the thermal unfolding of $tRNA^{Phe}$ at several salt concentrations are summarized in Table 8. In the temperature range and salt concentration covered in these studies, the unfolding of $tRNA^{Phe}$ was characterized by four separate transitions or five enthalpically distinct states. The additional high-termperature transition reported by Hinz et al.[21] lies outside the temperature range of these studies. According to these authors, the ΔH associated with this transition is equal to 58 kcal/mol and accounts for the observed differences in the overall enthalpy changes.

Freire and Biltonen[27] have previously shown that the experimental noise has negligible influence on the results of the deconvolution analysis, but erroneous determination of the temperature dependence of $C_{p,o}$ or an erroneous determination of the concentration of macromolecule in the calorimeter cell can influence the results of the analysis. Because the extrapolated baseline in these experiments is unusually long (~50°C), the possible effects of an incorrect baseline determination on the deconvolution results were examined. This was done by systematically varying the calculated temperature dependence of $C_{p,o}$ and repeating, in each case, the entire deconvolution analysis. This procedure is graphically illustrated in Figure 13, in which the two dotted lines represent the max-

TABLE 8

Deconvolution Analysis of the Thermal Unfolding of $tRNA^{Phe}$ (Yeast)

Transition	Δh[a] (kcal/mol)	[Na⁺] = 0.067 *M* T_m[b] (°C)	[Na⁺] = 0.067 *M* Δs[c] (cal/K·mol)	[Na⁺] = 0.17 *M* T_m[b] (°C)	[Na⁺] = 0.17 *M* Δs[c] (cal/K·mol)	[Na⁺] = 0.52 *M* T_m[b] (°C)	[Na⁺] = 0.52 *M* Δs[c] (cal/K·mol)
1	44 ± 2	33.4	144	37.0	142	41.4	140
2	61 ± 5	42.1	194	45.3	192	57.1	185
3	89 ± 10	48.5	277	54.0	272	62.1	266
4	73 ± 8	59.0	220	65.2	216	67.9	214

[a] From deconvolution analysis at three salt concentrations. (See text for details.) The values quoted are averages over three salt concentrations.

[b] From deconvolution analysis. $T_{m,i}$ is defined as the temperature at which $F_{i-1} = F_i$.

[c] $\Delta s_i = \Delta h_i / T_{m,i}$.

Taken from Freire, E. and Biltonen, R., *Biopolymers*, 17, 1257, 1978. With permission.

imal and the minimal slopes considered. The difference between these slopes is 30 cal/K²·mol and exceeds the experimental error with which the slope can be determined. The error in the calculated Δh was never greater than 10%, and the melting temperatures only slightly changed. In all cases, it was concluded that four transitions occurred over the experimental temperature interval. The influence of concentration errors up to 10% on the deconvolution results was also examined. A 10% error in the concentration introduces larger errors in the thermodynamic parameters than those introduced by the uncertainty in the extrapolated slope. However, these errors are still small and in no way affect the deduced thermodynamic characteristics of the transition.

Figure 14 shows the relative population of states, F_i, as a function of temperature for three different salt concentrations. As defined by Equation 39, the various F_i represent the average fraction of tRNA molecules populating a particular macroscopic energy state; in this sense, the population vs. temperature diagrams of intermediate states are characterized by bell-shaped functions which achieve a maximum and then decrease to zero as the next state becomes populated. For a sequential transition, the relative populations of the initial and final states are the only ones characterized by S-shaped curves. Since the excess heat-capacity function ($C_p - C_{p,o}$) is equal to the temperature derivative of the excess enthalpy function, $\langle \Delta H \rangle$, it follows that

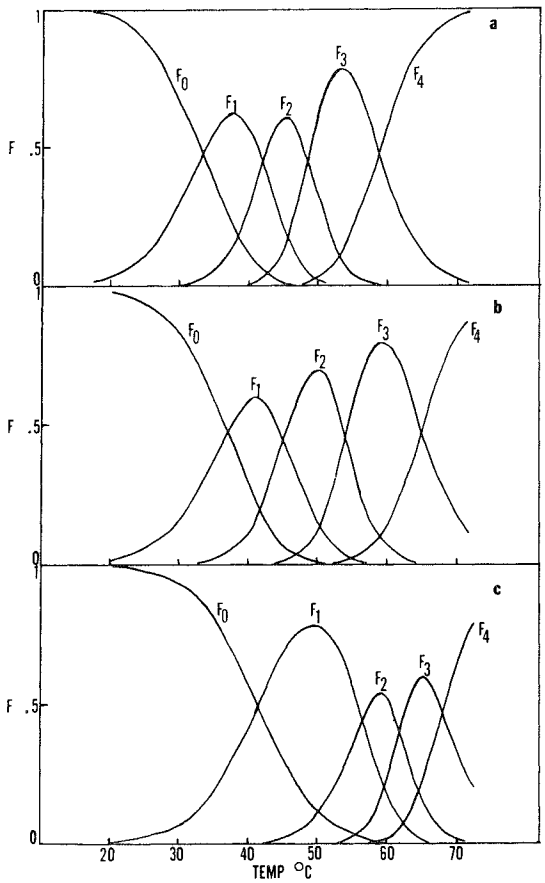

FIGURE 14. Relative populations vs. temperature of the five thermodynamic states associated with the thermal unfolding of $tRNA^{Phe}$ (yeast) in the temperature interval 0 to 72°C. (a: 0.067 *M* Na^+; b: 0.17 *M* Na^+; c: 0.52 *M* Na^+). (From Freire, E. and Biltonen, R., *Biopolymers*, 17, 1257, 1978. With permission.)

$$(C_p - C_{p,o}) = \sum_{i=1}^{n} \Delta H_i \frac{\partial F_i}{\partial T} + F_i \Delta C_{p,i} \qquad (57)$$

i.e., the contribution of each transition step to the overall C_p function is proportional to the derivatives $\partial F_i / \partial T$. This is illustrated in Figure 15 for the experiment at 0.067 *M* Na^+ and should be contrasted with the usual practice of approximating the overall heat capacity function by a collection of bell-shaped curves.

The Model of Independent Transitions as an Approximation to a Sequential Transition

Privalov et al.[20] and Hinz et al.[21] have analyzed the heat-capacity function of tRNA by fitting the experimental data to a theoretical curve which assumes that the sequential unfolding of tRNA can be approximated by a collection of independent noninteracting two-state processes in which each elementary process corresponds to the melting of a particular structural region of the molecule. There are several problems regarding this approximation which are circumvented by the deconvolution analysis. It is doubtful that the fitting of the heat-capacity function of tRNA to ten or more highly correlated variables can yield a unique solution, particularly since the estimation of the number of transitions to which the experimental curve is fit is arbitrary. The deconvolution analysis involves no fitting of the experimental data; the thermodynamic parameters of a sequential transition are obtained in a recursive form from the actual data, as has been shown. The deconvolution analysis yields directly the thermodynamic parameters of the transition and the number of macroscopic macromolecular energy states. Thus, the deconvolution results serve as a test for assessing the range of validity of a model of independent transitions as an approximation to a sequential transition.

The model of independent two-state transitions can provide reasonable estimates for the thermodynamic parameters of a sequential transition only when at any particular region of the independent variable, two consecutive macromolecular energy states are the only ones significantly populated and together account for ~100% of the total population of molecules. This situation is only realized when the individual transition steps are well separated on the temperature scale. Under these circumstances, the melting profiles of the sequential transition and the model of independent two-state transitions are identical and, therefore, thermodynamically indistinguishable.

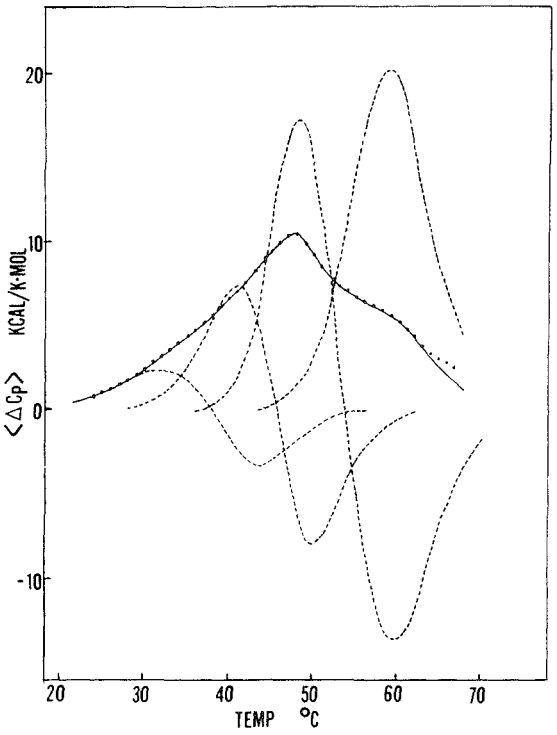

FIGURE 15. Apparent excess heat-capacity function of $tRNA^{Phe}$ (yeast) at 0.067 *M* Na^+. The solid line is the simulated curve by the deconvolution parameters. The experimental points have been plotted every 1°C. The dotted lines are the calculated contributions of each transition step to the overall heat capacity curve. The deviation between the calculated and experimental heat capacity curves at high temperature is real and is most likely associated with the beginning of the high-temperature transition reported by Hinz et al.[21] (From Freire, E. and Biltonen, R., *Biopolymers*, 17, 1257, 1978. With permission.)

As shown in Figure 14, this situation is never absolutely met in the transition region, particularly at high salt concentrations, in which transitions two, three, and four strongly overlap. Only at intermediate salt concentrations, where transitions two, three, and four are separated by 7 to 10°C, does the model of independent transitions provide reasonably good estimates for the thermodynamic parameters. It is in this salt concentration range that the enthalpies and melting temperatures calculated by Hinz et al.[21] qualitatively and quantitatively agree with the results of the deconvolution analysis.

It should be noted that the agreement between the parameters calculated by Hinz et al.[21] and the results of this analysis for the transition in 150 m*M* Na^+ does not imply that the various structural regions of $tRNA^{Phe}$ melt independently, but, rather, that under those particular salt conditions, the melting profiles associated with the model of independent transitions and the sequential transition coincide.

There is a fundamental difference between a sequential transition and a transition which is the sum of several independent two-state transitions, which is related to the total number of accessible macromolecular energy states. A sequential transition of n transition steps generates (n + 1) macromolecular energy states, but a collection of n independent two-state transitions will generate 2^n macromolecular energy states. If the n two-state transitions of the model of independent transitions are well separated in the temperature scale, only (n + 1) macromolecular states will be populated during the unfolding reaction, and the observed melting profile will be identical to that of a sequential transition. However, when the temperature spacing between transitions is small, the 2^n accessible states will progressively become populated, and the melting profile will be much broader than that expected from a sequential transition with the same parameters.

At high salt concentrations or in the presence of Mg^{2+}, in which the transition steps are closely spaced, the model of independent transitions for $tRNA^{Phe}$ does not provide sufficient cooperativity to account for the observed melting profiles. This model overcounts the number of accessible macromolecular energy states and, therefore, overestimates the entropy of the system. For this reason, this model cannot provide a consistent picture of the salt and Mg^{2+} dependence of the unfolding reaction. The sharpest heat-capacity profile attainable with this model will occur when all the $T_{m,i}$'s are the same; under these conditions, the heat-capacity maximum, $(\langle \Delta C_p \rangle)_{max}$, is given by

$$(\langle \Delta C_p \rangle)_{max} = \sum_i \frac{\Delta H_i^2}{4 R T_m^2} \qquad (58)$$

and the unfolding transition will exhibit a maximum in the heat-capacity curve of ~20 kcal/K/mol. $\langle \Delta C_p \rangle$ maxima larger than 20 kcal/K · mol are impossible to attain for the unfolding of $tRNA^{Phe}$, with a model of independent transitions. The peak maximum at 0.52 *M* Na^+ is of this order of magnitude, but the transition temperatures are dispersed over a temperature interval of about 25°C. In the presence of Mg^{2+}, $\langle \Delta C_p \rangle$ maxima of ~50 kcal/K · mol have been observed,[3,15] indicating that the effects of salt and Mg^{2+} cannot be interpreted by redistributing elementary two-state processes on the temperature scale.

The fact that the number of macromolecular states accessible to $tRNA^{Phe}$ remains unchanged up to salt concentrations of 0.52 *M* suggests the existence of intramolecular structural constraints which prevent the independent melting of the various structural regions of the molecule. The inclusion of the additional high-temperature transition reported by Hinz et al.[21] indicates that the total number of macromolecular energy states accessible to the $tRNA^{Phe}$ molecule in the absence of Mg^{2+} is six. This number is identical to that expected from the sequential melting of the tertiary structure and four helical regions of the molecule, but much smaller than the 32 allowed conformations expected from the independent melting of these structural regions. It thus appears that each branch of the tRNA molecule behaves as a single cooperative unit whose stability is determined by internal as well as intramolecular interactions. This conclusion is consistent with nuclear magnetic resonance studies[30] of intact tRNA and other studies on tRNA fragments which indicate that the thermodynamic stability of isolated regions is not the same as those observed in the whole molecule.[31]

Calorimetric evidence and the results of the deconvolution analysis indicate that the thermal unfolding of $tRNA^{Phe}$ is a sequential transition over the salt concentration range 0.067 to 0.52 *M*. These results also indicate that the assumptions made by Hinz et al.[21] for calculating the thermodynamic parameters of the transition are valid in the salt concentration range of their studies. However, those assumptions are incorrect when the transitions are closely spaced, as at high ionic strength or in the presence of Mg^{2+}. It thus appears that the deconvolution analysis described must be used if one wishes to accurately describe the conforma-

tional transitions of tRNA over a broad range of conditions.

GENERAL COOPERATIVE TRANSITIONS

In the preceding sections, the procedures were reviewed by which the partition function of a system could be calculated from the excess heat-capacity function, as well as how, in the case of the existence of distinct transitions, this information could be used to deduce the thermodynamic quantities associated with each transition. In many systems of biological interest (e.g., polypeptides, polyribonucleotides, DNA, and phospholipid bilayers), the individual macromolecular states differ only slightly in energy so that the discrete steps tend to merge into a near continuum of states. In such cases, it is not possible to deconvolute the transition curve into distinct transitions, but, having the partition function, it is possible to describe the overall thermodynamic changes and calculate molecular distribution functions. In these types of systems, the individual macromolecular states are not uniquely defined, and therefore a better description is obtained by considering the energy states accessible to a single residue (e.g., helix, coil, etc.). Macromolecular states are then defined in terms of statistical averages and distribution functions. Cooperative transitions are generally described by specifying the relative population of residues populating a particular energy state and the statistical distribution of such residues within the macromolecular moiety. This distribution of residues is not random but is constrained by the extent and magnitude of the cooperative interactions existing within the system. The greater the cooperativity, the greater the tendency of residues in the same state to group together, and, therefore, the smaller the probability of finding a pair of neighboring residues in different states. A highly cooperative transition is then characterized by the presence of large clusters or domains of residues in the same state. Conversely, in a poorly cooperative system, the size of these clusters tends to a minimum. A two-state transition as defined in previous sections is, within this context, a limiting case of a highly cooperative transition, i.e., one in which the probability of finding unlike neighbors is always zero.

Helix-coil transitions in polypeptide and polynucleotide systems, as well as the gel-liquid transition in phospholipid bilayers, are examples of these types of cooperative transitions. In these transitions, one is primarily interested in a precise evaluation of the fractional degree of melting, the relative population of residues in the various accessible energy states, and the statistical distribution of residues within the molecular array. The knowledge of this statistical distribution will provide information regarding the size of the clusters and the equilibrium fluctuations of the statistical averages.

This section will briefly summarize the basic theoretical background for the deconvolution analysis of cooperative transitions. The general theory for cooperative transitions in biopolymers has been continuously developed since the late 1950's, and excellent reviews exist.[38,50] The reader not familiar with this topic is referred to these references and the original references quoted in the text for a thorough discussion of the statistical mechanical concepts summarized here.

Recently, Freire and Biltonen[32] have shown that the statistical thermodynamic functions of cooperative systems can be directly deduced from excess heat-capacity data without requiring that the form of Q be specified by a precise model. This result thus opened the possibility of obtaining a statistical thermodynamic description of complex systems which heretofore has been extremely difficult.

This method is based upon the general result of statistical mechanics that in the thermodynamic limit canonical and grand canonical ensemble averages are identical.[33] For a system in which the macromolecule is composed of N identical units or residues (e.g., the amino acid residue comprising a polypeptide chain), a "residue partition function" can be defined as

$$q(N) = Q^{1/N} = \exp \int_{T_o}^{T} \frac{\langle \Delta h \rangle}{RT^2} dT \qquad (59)$$

where $\langle \Delta h \rangle \equiv \langle \Delta H \rangle / N$ is the excess enthalpy per mole of residues. As defined, the molecular partition function, Q, will always be recovered by raising q(N) to the N^{th} power. It is also true that as N becomes large, q(N) approaches a limit, q, in which it is independent of N. This situation defines the thermodynamic limit in

the canonical ensemble. It should be noted that Equation 59 provides a method for experimentally testing whether or not this limit has been reached.

The use of the grand canonical ensemble in relation with conformational transitions in macromolecules was introduced by Lifson and Zimm[34] for the helix-coil transition of DNA. Sture and Nordholm[35] provided a theoretical justification of its use and showed that if the thermodynamic limit exists in the grand canonical ensemble, then the molecular averages calculated from the canonical and grand cononical ensemble are identical for all the properties of the system that are bounded functions of N. The existence of the thermodynamic limit in the grand canonical ensemble is assured by the divergence condition of the grand partition function.

Making use of the formalism of the grand canonical ensemble, Freire and Biltonen[32] have shown that the molecular averages and distribution functions can be formulated in terms of experimental residue partition functions, which can be obtained from integration of the heat-capacity function. Thus, the molecular averages and distribution functions can be directly evaluated from experimental data, making possible the statistical thermodynamic analysis of transitions occurring in systems which are topologically of any dimension.

Clusters

Consider a molecular array of N units or residues, each of which can exist in two different states, A and B. A microscopic configuration of the system is specified by the fractional number of residues in states A and B and by the particular way in which these residues are distributed within the molecular lattice. This distribution of A and B residues will give rise to clusters of residues in state A and clusters of residues in state B. These clusters can be further specified by their average number and their average size as well as the relative fluctuations of these quantities around their mean value.

The total number of clusters, n_t, is

$$n_t = n_A + n_B \tag{60}$$

where n_A and n_B are the number of A and B clusters, respectively. If the number of A and B clusters having j residues is designated by $P_A(j)$ and $P_B(j)$, respectively, then the total number of residues in states A and B can be written as

$$N_A = \sum_{j=1} jP_A(j)$$

$$N_B = \sum_{j=1} jP_B(j) \tag{61}$$

and $N_A + N_B = N$.

The fraction of residues in states A and B is defined as

$$F_A = \frac{N_A}{N}$$

$$F_B = \frac{N_B}{N} \tag{62}$$

and the average size of clusters A and B by

$$\langle \ell_A \rangle = \frac{N_A}{n_A}$$

$$\langle \ell_B \rangle = \frac{N_B}{n_B} \tag{63}$$

The average properties of this system can be derived from the canonical partition function, $\mathcal{Z}(N)$, defined in Equation 27. By convention, state A is designated as stable at low temperatures and state B as stable above the transition temperature.

Next, the partition functions Q(N) and Z(N) are introduced. Q(N) is defined as the ratio between $\mathcal{Z}(N)$ and the statistical weight of the configuration in which $F_B = 0$. Z(N), on the other hand, is defined as the ratio between $\mathcal{Z}(N)$ and the statistical weight of the configuration in which $F_A = 0$. Z(N) and Q(N) differ only in the choice of the reference state; thus,

$$\frac{Z(N)}{Q(N)} = e^{-\Delta G^o/RT} \tag{64}$$

where $\Delta G^o = G_A - G_B$ is the free-energy difference between configurations A and B. The average thermodynamic properties of the system can be derived either from Z(N) or Q(N). The purpose of introducing Q(N) and Z(N) is that both functions can be experimentally evaluated; Q(N) by means of Equation 44 and Z(N) in an analogous form but performing the integration from the high- to the low-temperature end of the transition (Equation 47). Having

both quantities, one can evaluate ΔG° for the transition as a function of temperature.

Evaluation of the Partition Function

The canonical partition function, Z(N), can be evaluated by considering the grand partition function[32,34,36]

$$\Xi(\alpha) = \sum_N e^{-\alpha N} Z(N) \tag{65}$$

where α is the variable conjugate to the number of residues per macromolecule. α determines the average number of residues per macromolecule, <N>, and is specified by the condition

$$<N> = -\frac{\partial \ln \Xi}{\partial \alpha} \tag{66}$$

Considered as a power series, Equation 65 provides the basis for the sequence-generating function method originally proposed by Lifson.[37] Representing Equation 65 as

$$\Xi(x) = \sum_N x^{-N} Z(N) \quad (x = e^{\alpha}) \tag{67}$$

Lifson[37] has shown that $\Xi(x)$ converges for $x > x_1$, x_1 being defined as $x_1 \equiv [Z(N)]^{1/N}$, and diverges in the limit $x \to x_1$. Thus, x_1, and, therefore, Z(N), is the largest root of the equation $\Xi(x)^{-1} = 0$. This divergence condition also defines the thermodynamic limit of the grand canonical ensemble, i.e., the limit in which canonical and grand canonical averages coincide.

The Residue Partition Functions q and z

The experimental residue partition function q (Equation 59) is defined by the definite integral in which the integration is performed from the low- to the high-temperature end of the transition. For convenience, a second experimental residue partition function, z, ($z \equiv [Z(N)^{1/N}]$) obtained in an exactly analogous way to q but performing the integrations from the high- to the low-temperature end of the transition will be introduced. z is related to q by

$$\frac{z}{q} = e^{-\Delta g/RT} \equiv s \tag{68}$$

where $\Delta g = (g_A - g_B)$ is the free-energy difference per mole of residues in states A and B. It should be recognized that in the case of one-dimensional helix-coil transitions, the ratio $z/q \equiv s$ is identical to the helix-stability constant.

Since the canonical partition function Z(N) is, by definition, equal to z^N, it follows that in the thermodynamic limit

$$z = x_1 = e^{\alpha_o} \tag{69}$$

Grand Partition Function

Assuming that the clusters do not interact with one another or that the interactions are sufficiently weak such that the clusters can be considered as independent subsystems, the grand partition function Ξ can be written as a product of cluster grand partition functions[3] Ω_A and Ω_B:

$$\Xi = \sum_{\{n_A, n_B\}} (\Omega_A)^{n_A} (\Omega_B)^{n_B} \tag{70}$$

where the summation runs over all numbers of clusters. The cluster grand partition functions Ω_A and Ω_B are defined by the equations

$$\Omega_A = \sum_{j=1}^{\infty} g_A(j)\, e^{-j\alpha} \tag{71}$$

$$\Omega_B = \sum_{j=1}^{\infty} g_B(j)\, e^{-j\alpha} \tag{72}$$

where $g_A(j)$ and $g_B(j)$ are, respectively, the statistical weights or relative probabilities of finding A and B clusters containing j residues.

In the case of one-dimensional polymer chains, the grand partition function, Ξ, can be expressed in closed form due to the fact that the number of sequences n_A is always equal to n_B. Thus, Equation 70 becomes

$$\Xi = \sum_{n=0}^{\infty} (\Omega_A \Omega_B)^n$$

$$= (1 - \Omega_A \Omega_B)^{-1} \tag{73}$$

and diverges when $\Omega_A \Omega_B = 1$. This condition defines the thermodynamic limit in the grand canonical ensemble. In the case of two- and three-dimensional systems, however, no simple relation exists between n_A and n_B, and Ξ cannot be expressed in closed form.

Average Cluster Size

In the thermodynamic limit, the average sizes of clusters A and B are defined by:

$$\langle \ell_A \rangle = -\left(\frac{\partial \ln \Omega_A}{\partial \alpha} \right) \Bigg|_{\alpha = \alpha_0} \quad (74)$$

$$\langle \ell_B \rangle = -\left(\frac{\partial \ln \Omega_B}{\partial \alpha} \right) \Bigg|_{\alpha = \alpha_0} \quad (75)$$

or

$$\langle \ell_A \rangle = \frac{\sum_{j=1}^{\infty} j g_A(j)\, e^{-j\alpha_0}}{\sum_{j=1}^{\infty} g_A(j)\, e^{-j\alpha_0}} \quad (76)$$

$$= \frac{\sum_{i=1}^{\infty} j g_A(j)\, z^j}{\sum_{j=1}^{\infty} g_A(j)\, z^{-j}} \quad (77)$$

where z is the experimentally determined residue partition function. A similar expression holds for $\langle \ell_B \rangle$. At this point, a general closed expression for the average cluster sizes cannot be obtained because the statistical weights $g_A(j)$ are still undefined.

Helix-coil Transitions

Helix-coil transitions in polypeptide and nucleic acid systems are topologically one-dimensional transitions in which the molecular configurations of the polymer are specified in terms of alternating sequences of helix and coil residues. In the case of nucleic acid systems, coil sequences at internal positions of the polymer chain form matched or mismatched loops, depending on whether or not the number of coil residues in each strand of the loop is the same.[38]

Whereas the partition function for polypeptide models can be solved in closed form, this is not so for nucleic acid models. Difficulties arising from the mathematical form of the statistical weights of loops make impossible an exact solution for the partition function.[3] This fact is, however, immaterial from the point of view of the deconvolution analysis.

The statistical weight of a cluster (sequence) containing j residues in state A (helix) is simply s^j for both polypeptide and polynucleotide systems. In this case, Ω_A can be expressed in closed form as $\Omega_A = (q - 1)^{-1}$, and the average length of helical sequences, $\langle \ell_A \rangle$, can be immediately expressed as

$$\langle \ell_A \rangle = \frac{g}{g - 1} \quad (78)$$

and can be directly calculated from the experimental results.

Since the number of A(helix) and B(coil) sequences is the same, application of Equations 62 and 63 yields

$$\langle \ell_B \rangle = \langle \ell_A \rangle (1 - F_A) F_A^{-1} \quad (79)$$

so that only one statistical weight, $g_A(j)$ or $g_B(j)$, need be specified to experimentally obtain the average sequence lengths $\langle \ell_B \rangle$ and $\langle \ell_A \rangle$. This is a completely general result from transitions occurring in topologically one-dimensional spaces. Furthermore, the statistical weight, s, can be experimentally obtained using Equation 68. In what follows we will assume that $g_A(j) = s^j$; however, the formalism will remain the same for any other functional form of $g_A(j)$.

The fraction of residues in states A or B is directly related to the average excess enthalpy $\langle \Delta h \rangle$:

$$F_B = \frac{N_B}{N} = \frac{\langle \Delta h \rangle}{\Delta h} \quad (80)$$

$$F_A = \frac{N_A}{N} = 1 - F_B \quad (81)$$

where $\langle \Delta h \rangle$ and Δh are expressed in energy units per mole of residue. Having F_A and F_B and $\langle \ell_A \rangle$ and $\langle \ell_B \rangle$, one can calculate the average number of A and B clusters from

$$\frac{F_A}{\langle \ell_A \rangle} = \frac{n_A}{N}$$

$$\frac{F_B}{\langle \ell_B \rangle} = \frac{n_B}{N} \quad (82)$$

Distribution Functions and Fluctuations

Up to this point, we have been primarily concerned with the derivation of the appropriate expressions for the thermodynamic molecular averages. A detailed molecular picture of the system requires the knowledge of the distribution functions leading to the macroscopic averages. This information is also contained in the partition function.

Consider first the probability functions associated with the residues in state A (an analogous

treatment will lead to the functions associated with the residues in state B.) The probability, $P_A(\ell)$, of finding a cluster of residues in state A containing ℓ residues among all A clusters is

$$P_A(\ell) = \frac{s^{\ell} e^{\alpha_0}}{\Omega_A} \quad (83)$$

and can be expressed in terms of the experimental residue partition function, q, as

$$P_A(\ell) = \frac{q-1}{q^{\ell}} \quad (84)$$

The moment-generating function of the distribution is

$$<\ell_A^k> = \sum_{\ell=1}^{\infty} \ell^k P_A(\ell) \quad (85)$$

and can be expressed in terms of q as

$$<\ell_A^k> = (q-1) \sum_{\ell=1}^{\infty} \ell^k q^{-\ell} \quad (86)$$

thus allowing us to express all the moments of the distribution in closed form. The first moment is equal to the average cluster size, $<\ell_A>$. The second moment, $<\ell^2_A>$, equal to

$$<\ell_A^2> = \frac{q(q+1)}{(q-1)^2} \quad (87)$$

provides a measure of the breadth of the distribution. The dispersion, Δ^2, can be expressed in terms of the first and second moments as

$$\Delta^2 = <\ell_A^2> - <\ell_A>^2 = <\ell_A>(<\ell_A> - 1) \cong <\ell_A>^2$$

and indicates a relatively broad distribution with a root mean square deviation approximately equal to the average cluster size. The magnitude of the equilibrium fluctuations in cluster size is give by Δ.

Another quantity of interest is the probability, $\rho_A(j)$, that an A residue picked at random is in a cluster of j residues:

$$\rho_{A(j)} = \frac{jp_{A(j)}}{\Sigma jp_{A(j)}} = \frac{j(q-1)^2}{q^{j+1}} \quad (89)$$

The generality of the above treatment can be verified by replacing q by the appropriate expression corresponding to one of the different models existing in the literature. For example, if the value $q = 1 + \sigma^{1/2}$, corresponding to the nearest-neighbor Ising model at $s = 1$, is replaced in Equation 89, it reduces to the expression derived by Poland and Scheraga[38] by a rather different approach. An extensive discussion of this quantity as well as some approxximate treatments are given in the same reference.

The residue partition functions, q and z, are in the context of the deconvolution theory, thermodynamically defined so that their calculation from experimental data does not require any special assumptions regarding the nature or mechanism of the transition other than that the system can be approximated as being infinite in size. q or z can be used for experimentally testing whether or not the infinite size limit has been reached at some large, but still finite, degree of polymerization, N. In this limit which defines the thermodynamic limit in the canonical ensemble, the residue partition functions, q and z, are independent of N. As the degree of polymerization, N, becomes very large, q and z should asymptotically approach a limiting value.

ANALYSIS OF HELIX-COIL TRANSITIONS IN HOMOPOLYMERS

In the preceding section, the formalism for statistical mechanical analysis of conformational transitions of highly cooperative homogeneous polymers was reviewed. The simplest system to which to apply this procedure is the helix-coil transition of polypeptides. Evaluation of q and z as described will yield s, the helix stability constant, and complete distribution functions of helical lengths, etc., as functions of temperature. However, the results of such an analysis of polypeptides will not be presented; instead, the behavior of double-strand to single-strand transitions of polynucleotides will be immediately considered. This system is more complex because strand separation occurs and because both unraveling at the ends and formation of internal loops can occur. The deconvolution theory for this class of systems has been developed in Reference 40. In this section, those results will be reviewed.

A double-strand to single-strand transition can be represented as

$$ {}_2I_0 \underset{}{\overset{K_1}{\rightleftharpoons}} {}_2I_1 \overset{K_2}{\rightleftharpoons} {}_2I_2 \cdots\cdots {}_2I_{n-1} \overset{K_n}{\rightleftharpoons} {}_1I_n \qquad (90) $$

where all species up to ${}_2I_{n-1}$ inclusive are double-stranded forms characterized by different degrees of base pairing and ${}_1I_n$ representing all the possible forms of the single-stranded conformation. Here ${}_xI_y$ refers to a species of x strands with y broken base pairs. The partition function, Q, of this system is represented by

$$ Q = 1 + \sum_{i=1}^{n} \omega_i \, e^{-\Delta G_i / RT} \qquad (91) $$

the concentration dependence for double-strand formation being included in the last term of the summation. The residue partition function per base pair, q, defined as $q \equiv Q^{1/N}$ (where N is the average degree of polymerization of the double-stranded molecule) is the quantity directly obtained from the experiment since the polymer concentration is always determined in moles of nucleotides; additional knowledge of the polymer molecular weight allows calculation of Q. The fraction of molecules in the i^{th} state, defined as

$$ F_{i \neq n} = \frac{({}_2I_i)}{({}_2I_0) + ({}_2I_1) + \cdots\cdots + ({}_1I_n)/2} $$

$$ F_n = \frac{({}_1I_n)}{2\{({}_2I_0) + ({}_2I_1) + \cdots\cdots + ({}_1I_n)/2\}} \qquad (92) $$

is given by

$$ F_i = \frac{e^{-\Delta G_i / RT}}{Q} \qquad (93) $$

and together with the partition function can be calculated with the deconvolution equations given in the section on multistate transitions.

The overall fraction, $(\theta_h)_t$, of base pairs is assumed to be

$$ (\theta_h)_t = \frac{\Delta H - \langle \Delta H \rangle}{\Delta H} \qquad (94) $$

and the fraction θ_h of base pairs among the double-stranded molecules

$$ \theta_h = \frac{(\theta_h)_t}{(1 - F_n)} \qquad (95) $$

At any temperature, the fraction of single-stranded molecules (F_n) can be calculated by means of the relation

$$ F_n = \exp\left(-\int_{T}^{T_n} (\Delta H_n - \langle \Delta H \rangle) \frac{1}{RT^2} \, dT\right) \qquad (96) $$

where the enthalpy terms are given in calories per mole of double-stranded molecules. The average excess enthalpy of the system $\langle \Delta H \rangle$ is

$$ \langle \Delta H \rangle = \sum_{i=0}^{n-1} F_i \Delta H_i + F_n \Delta H_n \qquad (97) $$

from which the average excess enthalpy function associated with the double-stranded molecules ($\langle \Delta H \rangle^*$) can be calculated,

$$ \langle \Delta H \rangle^* = \frac{\sum_{i=0}^{n-1} \Delta H_i e^{-\Delta G_i / RT}}{Q^*} \qquad (98) $$

$$ = \frac{\langle \Delta H \rangle - F_n \Delta H}{1 - F_n} \qquad (99) $$

Q is the partition function for double strands only, which is numerically obtained from the equation

$$ Q^* = \exp\left(\int_{T_o}^{T} \frac{\langle \Delta H \rangle^*}{RT^2} \, dT\right) \qquad (100) $$

The strand separation step in the general reaction mechanism is analytically isolated from the whole transition, according to the equilibrium

$$ \sum_{i=0}^{n-1} {}_2I_i \rightleftharpoons 2\,{}_1I_n \qquad (101) $$

with equilibrium constant, K, defined as

$$ K = \frac{(I_n)^2}{\sum_{i=0}^{n-1} (I_i)} $$

$$ K = \frac{2 C_t F_n^2}{(1 - F_n)} \qquad (102) $$

where C_t is the total concentration of polymeric molecule expressed in moles of single-stranded forms. The apparent enthalpy change for the strand separation, defined in terms of the classical van't Hoff equation, is

$$\Delta H_{VH} = -R \frac{d \ln K}{d\ 1/T} = \Delta H_n - \langle \Delta H \rangle^* \quad (103)$$

where ΔH_n is the total heat for the transition and $\langle \Delta H \rangle^*$ the average excess enthalpy per mole of double-stranded form at the point in which the strand separation occurs. If the usual assumption that the main contribution to the total enthalpy change is the disruption of base pairs is made, it follows that

$$\Delta H_{vh} = \Delta h\,(N - \langle n \rangle^*) \quad (104)$$

where Δh is the enthalpy change associated with breaking one base pair, N the total number of base pairs per polymer chain, and $\langle n \rangle^*$ the average number of broken base pairs in the double-stranded chain immediately before the strand separation. In other words, $(N - \langle n \rangle^*)$ is a measure of the size of the cooperative unit required for the formation of the double-stranded polymer.

A typical excess heat-capacity curve for a mixture of double-stranded poly(A) · poly(U) is shown in Figure 4. The average excess enthalpy function, $\langle \Delta H \rangle$, was calculated by integration of the quantity $(C_P - C_{P,o})$ as described. The heat capacity of the initial state, $C_{P,o}$, was calculated by a linear least-squares fit of the initial part of the apparent heat-capacity curve (generally between 10 and 20°C) and extrapolated over the entire transitional interval. With this procedure, an average ΔC_p difference of 91 ± 8 cal/K/mol base pairs between the final and initial state was obtained. For this particular experiment, ΔH was calculated to be 6.8 kcal/mol base pair.

Having $\langle \Delta H \rangle$, the partition function, Q, was calculated as described, assuming 450 base pairs per polymer complex. The partition function $Z \equiv z^N$ was calculated in an analogous way to Q but performing the integrations from the high- to the low-temperature ends of the transition. In Figure 16, the fraction of broken base pairs and the fraction of single-stranded molecules, F_n, are plotted as a function of temperature. In calculating F_n, a total average number of 450 base pairs per double-stranded molecule was assumed; the effect of increasing or decreasing this number plus or minus 100 nucleotides was only to shift the F_n curve ±0.1°C on the temperature scale.

In Figure 17, the temperature dependence of the strand separation equilibrium constants is shown. The equilibrium constants were calculated by means of Equation 103 and the corresponding van't Hoff enthalpy change calculated by a linear least-squares fit. The results are summarized in Table 9. The linearity of the van't Hoff plots indicates a basic homogeneity in the size of the cooperative unit, suggesting that the experimental data are not significantly affected by the slight length heterogeneity of the polymer sample.

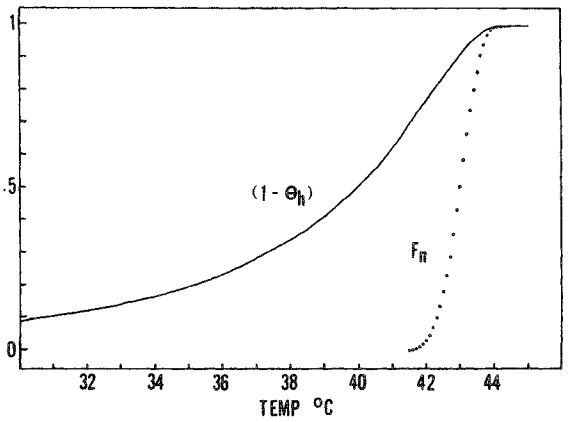

FIGURE 16. Experimental fraction of broken base pairs, $(1 - \theta_h)$ [solid line], and fraction of single stranded molecules, F_n, vs. temperature, for the helix-coil transition of poly(A) · poly(U) at $[Na^+] = 0.016$ *M*. (From Freire, E. and Biltonen, R., *Biopolymers*, 17, 497, 1978. With permission.)

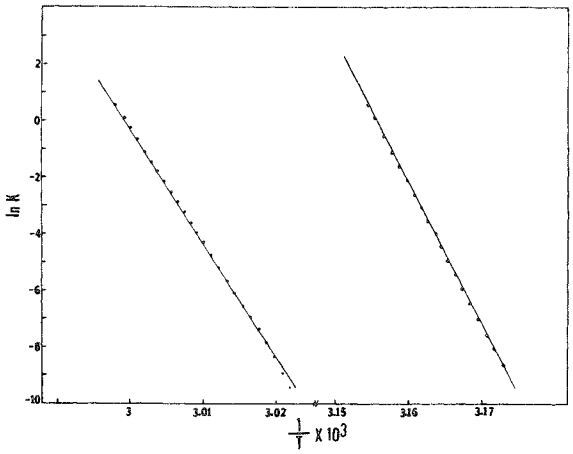

FIGURE 17. Van't Hoff representation of the strand separation equilibrium constant, K, at $[Na^+] = 0.016$ *M* and $[Na^+] = 0.16$ *M*. The results of a linear least-squares analysis are summarized in Table 9. (From Freire, E. and Biltonen, R., *Biopol ymers*, 17, 497, 1978. With permission.)

TABLE 9

Thermodynamic Parameters Characterizing the Strand Separation of Poly(A) · Poly(U)

[Na⁺][a]	$T_{m,n}$ (°C)[b]	$(\Delta F/\Delta T)^{-1}$ (°C)[c]	ΔH_{vh}[d]	(N−<n>*)[e]
0.016*M*	43.0±0.1	1.3	980±80	144±12
0.16 *M*	59.3±0.1	1.5	880±80	114±11

[a] Total Na^+ concentration.
[b] Temperature at which the fraction of single-stranded molecules, F_n, is 0.5.
[c] Transition breadth (see text for details).
[d] kcal/mol double-stranded molecules.
[e] Cooperative unit size for strand separation.

Taken from Freire, E. and Biltonen, R., *Biopolymers*, 17, 497, 1978. With permission.

Although the midpoint temperature of the strand separation transition was found to be strongly dependent on salt concentration ($\Delta T_m/\Delta \ln Na = 7.62$), the basic characteristics of the transition remain unchanged over a tenfold range in the salt concentration.[40] These sharp transitions are characterized by a transition breadth (defined as the reciprocal of the transition slope at T_m) of 1.4 ± 0.1°C. At [Na^+] = 0.016 *M*, the van't Hoff enthalpy is consistent with the disruption of 144 ± 12 base pairs, whereas at [Na^+] = 0.16 *M*, it is consistent with the disruption of 114 ± 11 base pairs. These results provide the thermodynamic characterization of the double-strand → single-strand transition at T_m.

As discussed in the preceding section, the base-pair partition functions, q and z, differ only in the choice of the reference state, so that the ratio z/q is equal to the helix stability constant, s. Having experimentally determined q and z as continuous functions of temperature, one is able to calculate s over the whole temperature interval of the transition. It is interesting to note that a direct determination of s has never before been possible, even though it has the simple form of an equilibrium constant, and that very precise calorimetric enthalpy values exist in the literature. The major difficulty arises in evaluating T_s, the temperature at which = 1. Up to now, T_s has been only theoretically estimated or left as an adjustable parameter to the obtained from the fitting of the overall experimental melting profile to a predefined model.[39,41]

According to the formalism developed, s is obtained from the experimental data without assuming a particular model for the transition. This capability of the deconvolution analysis was tested by performing a van't Hoff analysis of the quantity ln(z/q). The results are shown in Figure 18. A linear least-squares analysis of the data yielded apparent enthalpies for base-pair formation of −6.5 kcal/mol and −7.6 kcal/mol, respectively, which are in excellent agreement with the overall enthalpy changes calculated from the area under the C_p curves. From this analysis, it was found that the stability constant is equal to unity when the fraction of remaining base pairs (θ_h) is equal to 0.7 and 0.65 at [Na^+] = 0.016 *M* and [Na^+] = 0.16 *M*, respectively. Comparable values have been previously estimated from calorimetric[16] ($\theta_h \simeq 0.7$ at s = 1) and spectrophotometric[41] ($\theta_h \simeq 0.75$ at s = 1) data.

These results rule out the zipper and staggering zipper models as plausible approximations for the transitions of these long polymeric chains. If these transitions were described by either of these two models, θ_h would be equal to 0.33 and 0.25 at s = 1, respectively. Since $\theta_h \simeq 0.7$ at s = 1, the transition must proceed through the formation of internal loops of coil residues. This is to be expected from theoretical considerations and is a reflection of the fact that the entropy of a loop is smaller than that of an open sequence at one end of the chain having the same number of coil residues.

Average Sequence Lengths

In Figure 19, the calculated average helical and coil sequence lengths have been plotted as

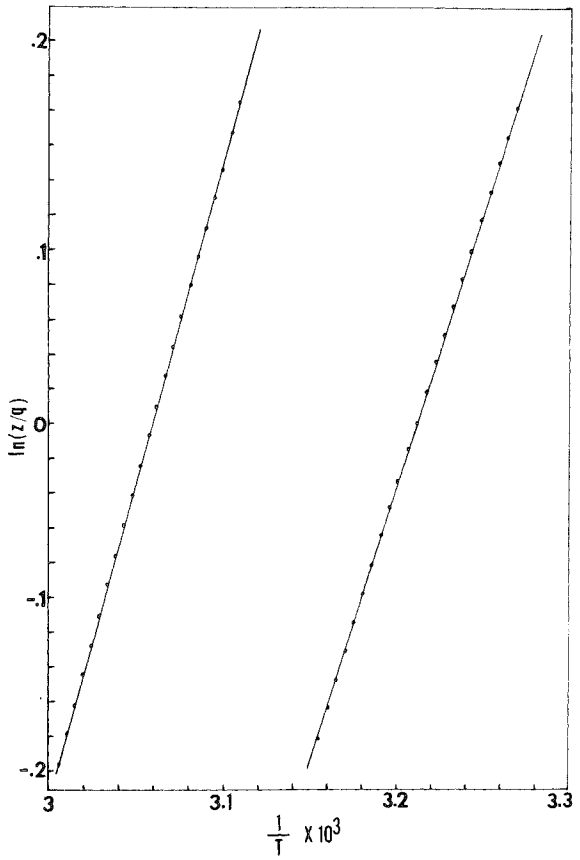

FIGURE 18. Van't Hoff representation of ln (z/q) for the helix-coil transition of poly(A) · poly(U) at [Na⁺] = 0.06 *M* and [Na⁺] = 0.16 *M*. According to the theory, ln (z/q) is equal to ln s, where s is the helix stability constant. See text for details. (From Freire, E. and Biltonen, R., *Biopolymers*, 17, 497, 1978. With permission.)

a function of θ_h for the experiment at 0.016 *M* Na^+. The mean coil length remains practically constant for values of $\theta_h > 0.5$, whereas the average helical length decreases with θ_h. In all the experiments, the helical length dropped to about 10% of the polymer length before the number of broken base pairs reached 20% of the total. This melting pattern can only occur when a significant amount of broken base pairs are at internal positions of the polynucleotide chain and not only at the ends of the molecule. If there were a single helical sequence whose melting proceeds from the ends, then the mean coil length would monotonically increase at a rate proportional to the decrease in the mean helical length.

For values of $\theta_h < 0.5$, the mean coil length grows at a rate which is faster than the decrease

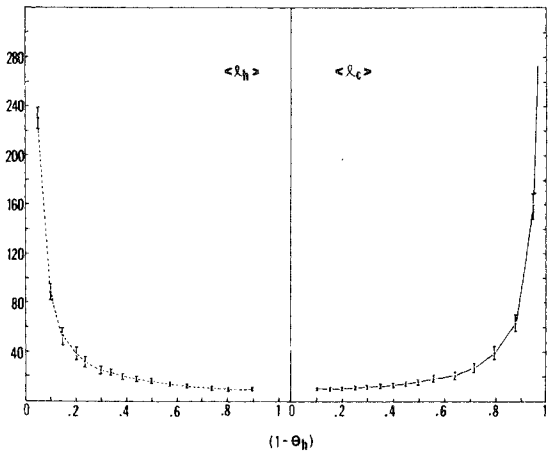

FIGURE 19. Experimental average helical and coil sequence lengths ($<\ell_h>$ and $<\ell_c>$) associated with the helix-coil transition of poly(A) · poly(U) at [Na⁺] = 0.016 *M*. (From Freire, E. and Biltonen, R., *Biopolymers*, 17, 497, 1978. With permission.)

in mean helical length and appears to asymptotically approach a final finite value of ~10 base pairs at the critical region in which the strand separation occurs. In this region, the increase in the average coil length is not correlated with a further decrease in the mean helical length but, rather, with a reduction in the total number of helical segments. This phenomenon is illustrated in Figure 20, in which the average number of helical sequences is plotted vs. the average coil length. Applequist has argued on theoretical grounds[39] that a critical helical length might exist beyond which the melting proceeds at the expense of the number of sequences, but with little change in the size of the helices. These experiments confirm his predictions. It is to be noted that the critical helical length in the double-stranded form is substantially less than the average number of base pairs per double-stranded polymer at the transition temperature (120).

These results clearly demonstrate the usefulness of the deconvolution analysis in providing the necessary information for a complete statistical thermodynamic characterization of double-stranded and single-stranded transitions of polynucleotides. This method allows a direct determination of the average molecular properties of the polymer, without assuming a particular expression for the statistical weights of coil residues at internal positions of the chain The above calculations do not require any

priori estimation of the base-stacking parameter and the loop closure exponent. This should be an advantage in dealing with samples of heterogeneous base composition.

ORDER-DISORDER TRANSITIONS IN PHOSPHOLIPID BILAYERS

The excess heat-capacity function of multilamellar DPPC liposome was shown in Figure 7. The nature of the smaller, low-temperature transition is not yet well understood, and the $<\Delta C_p>$ curve for this transition very likely does not represent an equilibrium situation.[11] The main transition at 41.3°C is known to involve loss of regular order of the hydrocarbon chains and is often referred to as a "gel-liquid crystalline" phase transition. It is this transition upon which the current discussion will focus.

These gel-crystalline phase transitions have been studied with several experimental techniques, including scanning calorimetry,[11,23-25] fluorescence probes,[11] NMR,[42] X-ray scattering,[43] and density measurements.[44] These works have shown that the thermodynamic characteristics of this transition are greatly altered by changing the phospholipid chain length, increasing the radius of curvature of the vesicle, and adding compounds with a small molecular weight, such as anesthetics, to the system. Several workers have considered various statistical mechanical models to describe this transition in phospholipid bilayers. However, the work has been primarily directed towards formulating plausible expressions for the possible configurational states of the hydrocarbon chains of the phospholipids and not for the conformational states of the bilayer as a whole.

Although it is recognized that the properties of the bilayer have their ultimate origin in the configurational state of the phospholipid molecules, there does not appear to be a simple one-to-one correspondence between the properties of the bilayer and their isolated constituents. For example, there is strong experimental evidence which indicates that transport properties across the membrane do not directly depend on the degree of fluidity of the phospholipids. This and similar phenomena do not appear to be simply correlated to the degree of fluidity of the bilayer or the average conformational state of the phospholipids. It thus appears that important properties of the bilayer depend not only on the average degree of fluidity but on the organization and distribution of the phospholipids within the bilayer. Therefore, in studying the properties of the bilayer, one should not only be concerned with the physical state of the phospholipids but with the rules by which the average properties of the bilayer are defined.

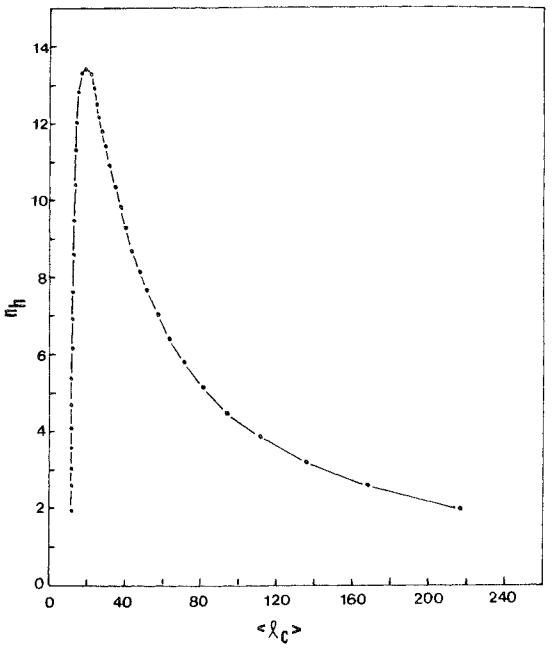

FIGURE 20. Experimentally determined average number of helical sequences vs. average coil length. This figure clearly demonstrates that the last step in the helix-coil transition is made at the expense of reducing the total number of helical sequences, but with little change in the size of the helical segments. (From Freire, E. and Biltonen, R., *Biopolymers*, 17, 497, 1978. With permission.)

In analogy to the situation for synthetic polypeptides and polynucleotides which are topologically one dimensional, the bilayer can be thought of as being formed of clusters of phospholipids in the gel state and clusters of phospholipids in the liquid crystal state. At temperatures well below the transition temperature, T_m, all the phospholipids are in the gel state. At temperatures well above T_m, the entire bilayer can be considered as being a single liquid crystal cluster. In the transition region, the state of the bilayer can be described by a particular distribution of clusters of phospholipids in the gel state and clusters of phospholipids in the liquid crystal state.

Freire and Biltonen[32] have developed the theoretical groundwork for the statistical thermodynamic description of a cooperative transition in terms of cluster distribution functions and some operational relations which allow calculation of those functions from scanning calorimetric data. Regarding a hypothetical bilayer at the transition midpoint (i.e., when half of its phospholipids are in the gel state and half in the liquid crystal state), it is significant to ask what is the configurational state of the whole bilayer at that point. The sole specification of the fraction of phospholipids melted does not provide much information on the state of the bilayer; there are a very large number of configurations which satisfy the restriction that the fraction of phospholipids melted is one half. A more detailed description of the bilayer would be obtained if the cluster distribution functions were known. Then, the relative fluctuation of the averages and the probability of finding a cluster of any particular size could be defined.

Each phospholipid molecule which melts during the transition can create a new liquid crystal cluster of unit size, increase the size of a preexisting cluster by one, or join two (or more) already existing clusters. The relative probability of occurrence of any of these events will depend on the magnitude of the cooperative interactions existing within the bilayer and the fractional degree of melting.

The gel-liquid crystal transition is highly cooperative; cooperativity is defined simply as the tendency of the residues in the same state to group together. The actual nature of the transition (which lies somewhere between the noncooperative and infinitely cooperative cases) will depend on the ultimate balance between two forces, the combinatorial entropy which tends to maximize the number of clusters, minimizing their size, and the cooperative forces which tend to maximize the cluster size, minimizing their number. The former has its origin in the combinatorial degeneracy and is entropic in nature. The latter, on the other hand, could arise from different kinds of interactions, whose origin, within the bilayer, is still unknown. For example, the model of Jackson[45] for the conformation of the hydrocarbon chains assumes that a source of cooperativity is the energy difference between what he refers to as a "forcing kink" and a "falling kink." In any case, cooperative interactions cause gel-gel or liquid-liquid neighbors to be energetically more favorable than gel-liquid neighbors.

The shape of a gel-liquid crystalline transition curve will be defined by the enthalpy of melting of the phospholipid molecules and the magnitude of cooperative interactions. Several variables or perturbations to the system can affect one or both of these basic types of interactions. For example, Suurkuusk et al.[11] have demonstrated that changes in the radius of curvature of DPPC liposomes affect the total enthalpy change, and Mountcastle et al.[46] have demonstrated that the presence of the gaseous anesthetic, halothane, reduces the degree of cooperative interaction without significantly affecting ΔH. In this discussion, the latter example will be used as the basis for considering the analysis of $\langle \Delta C_p \rangle$ data to obtain statistical mechanical information regarding the transition.

In Figure 21, the excess heat-capacity function, $\langle \Delta C_p \rangle$, of an aqueous dispersion of multilamellar liposomes prepared from DPPC in the absence and in the presence of 4.7% atm of the anesthetic halothane is plotted. In the absence of the anesthetic, the main transition of DPPC is characterized by a melting temperature, T_m, of 41.3°C and a calorimetric ΔH of 8.6 kcal/mol of phospholipids. In the presence of the anesthetic, T_m is lowered to 39.5°C and the calorimetric ΔH was found to equal 7.8 kcal/mol. However, the most dramatic change is in the cooperativity of the transition. In the absence of the anesthetic, the half height-width of the transition is only 0.5°C, whereas, in the presence of the anesthetic, it is broadened to 2°C. These two experiments were chosen for the purpose of this discussion because the anesthetic predominantly affects the cooperativite of the transition, leaving unchanged other properties of the bilayer.

The quantities directly accessible from scanning calorimetry are the residue partition functions, q and z, defined as before. In calculating q, the state that is stable below the transition temperature (gel) is taken as reference states whereas in calculating z, the state that is stable above the transition temperature (liquid crystal is the reference state. The ratio z/q is equal to

$$s \equiv \frac{z}{q} = e^{-\Delta g/RT}$$

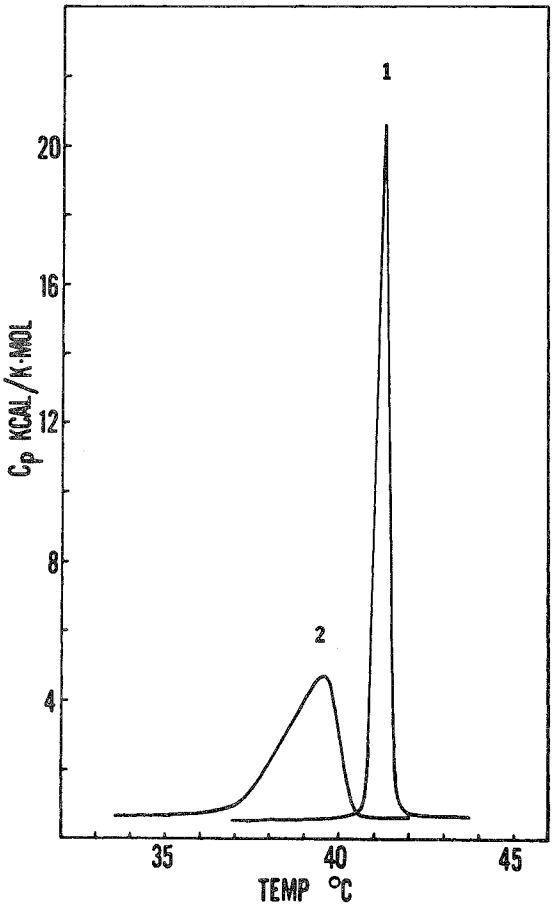

FIGURE 21. Heat capacity function associated with the main transition of a fresh dispersion of: (1) multilamellar lipos mes prepared from pure DPPC and (2) multilamellar liposomes prepared from DPPC in the presence of 4.7 atm of the gaseous anesthetic, halothane.

where Δg is the free energy difference between the gel and liquid crystal states ($\Delta g = g_{gel} - g_l$) per mole of phospholipid. This relation allows calculation of Δg as a continuous function of temperature without making any assumption about the mechanism of the transition.

The van't Hoff representation of the quantity $s \equiv z/q$ is shown in Figure 22 for these two experiments. The results of a linear least-squares analysis are summarized in Table 10. The agreement between the Δh values obtained in this form and those calculated from the area under the C_p curve is very good. It should be noted that the temperature at which Δg is zero is not equal to the temperature of the maximum in $\langle \Delta C_p \rangle$. This is particularly noticeable for the transition in the presence of halothane. This effect is not due to experimental error in the de-

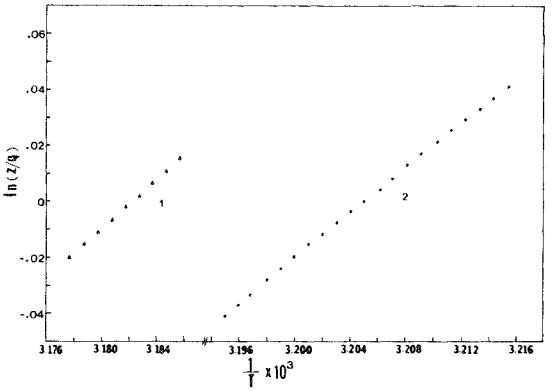

FIGURE 22. Van't Hoff representation of ln (z/q) for the gel-liquid crystalline transition of multilamellar DPPC liposomes in the absence (1) and in the presence (2) of 4.7 atm of halothane. The results of a least-squares analysis are shown in Table 10.

termination of Δg but merely reflects the fact that the transitions are not perfectly symmetrical. For an assymetrical transition, T_m (defined as the position of the maximum in $\langle \Delta C_p \rangle$) is not equal to the temperature at which $\Delta g = 0$, and, in general, no simple relation exists between the position of the maximum and the value of Δg at that point. The deconvolution method thus provides a unique opportunity of having a direct experimental access to Δg, without a priori assuming a model for the transition.

Freire and Biltonen assumed that this system is sufficiently large so that the residue partition functions, q and z, are independent of N, the average number of residues per liposome. This assumption appears justified in the case of multilamellar liposomes. The above assumption does not impose any restriction on the dependence of q and z on the length of the hydrocarbon chains. In this treatment, q and z are obtained from the experimental data, and, thus, no assumptions about their internal structure are required. This is to be contrasted with the so-called *ab initio* models in which the hydrocarbon partition functions need to be solved. The residue partition functions, q and z, as effective partition functions, contain contributions from the configurational state of the phospholipids as well as contributions from the interactions arising from the particular way in which the phospholipids are organized within the bilayer.

If the reference state is defined as that state

TABLE 10

Thermodynamic Parameters Associated with the Gel-liquid Crystal Transition of DPPC[a]

System	Δh (kcal/mol)[b]	T_m (°C)[c]	Δh_{vh} (kcal/mol)[d]	$(T_m)_{\Delta g = 0}$ (°C)[e]
DPPC	8.6	41.3	8.59	41.25
DPPC + 4.7% halothane	7.8	39.5	7.92	39.0

[a] Multilamellar liposomes prepared from DPPC.
[b] Calorimetric Δh: area under the $<\Delta C_p>$ curve.
[c] Temperature of the maximum value in $<\Delta C_p>$.
[d] From van't Hoff analysis of $\ln \frac{z}{q} = \ln s$. See text for details.
[e] Temperature at which $\Delta g = 0$.

of the bilayer which is stable above the transition temperature (i.e., the state in which all the phospholipids are in the liquid crystal state), the statistical weight of a phospholipid in the gel state relative to a phospholipid in the liquid crystal state is s, the equilibrium constant for the conversion of a phospholipid from the liquid state to the gel state. Note that s, defined as z/q, is not the equilibrium constant for the conversion of an isolated phospholipid but, rather, the effective equilibrium constant per phospholipid when this process occurs within the bilayer; therefore, s already includes the interaction energies existing in the bilayer, and no further specifications are required to define the statistical weight g_{gel} (j). The gel cluster grand partition function, Ω_{gel}, is given by Equation 71, and the average size of gel clusters, $<\ell_{gel}>$, is given by Equation 78. In Figures 23 and 24, the $<\ell_{gel}>$ calculated from the $<\Delta C_p>$ functions of Figure 21 has been plotted as a function of the degree of melting. The cluster densities n_{gel}/N are also shown.

In writing the statistical weight of a liquid crystal cluster, one needs to consider two kinds of phospholipids, those surrounded by other molecules in the liquid state and those existing at the boundaries of the cluster, which are also in contact with phospholipids in the gel state.

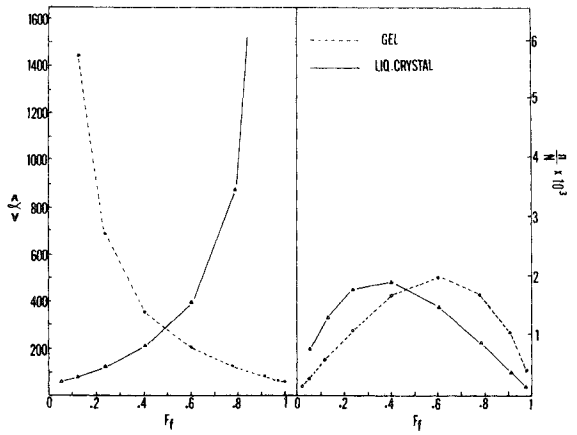

FIGURE 23. Cluster averages associated with the gel-liquid crystalline transition of pure multilamellar DPPC liposomes: (A) experimental average gel and liquid cluster size ($<\ell_g>$ and $<\ell_{ff}>$) as a function of the fraction of phospholipids in the liquid state, F_f; and (B) experimental gel and liquid cluster densities (n_g/N and n_{ff}/N) as a function of F_f.

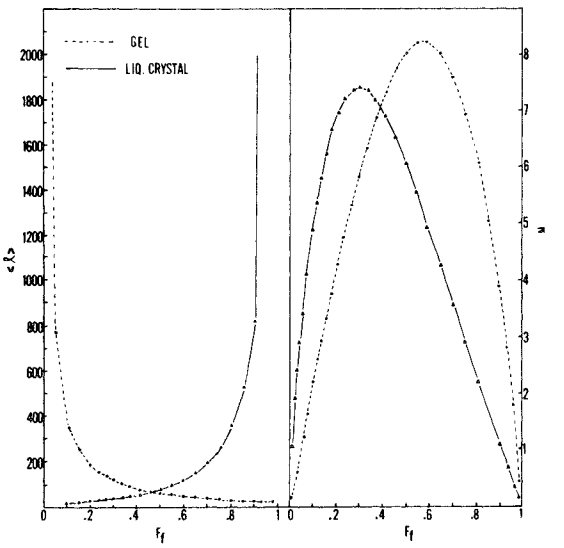

FIGURE 24. Cluster averages associated with the gel-liquid crystalline transition of multilamellar DPPC liposome in the presence of 4.7 atm halothane: (A) experimental average gel and liquid cluster size ($<\ell_g>$ and $<\ell_{ff}>$) as a function of F_f and (B) experimental gel and liquid cluster densities (n_g/N and n_{ff}/N) as a function of F_f.

As mentioned before, cooperative interactions cause the molecules at the interphase region to be energetically less stable than those surrounded by molecules in the same state. This interfacial region is considered to be the outer layer of a liquid crystal cluster; analogous results would be obtained if this convention were inverted. The liquid crystal cluster grand partition function, Ω_f, is, then,

$$\Omega_f = \sum_{j=1}^{\infty} \lambda^{m(j)} e^{-j\alpha} \tag{106}$$

where λ is the statistical weight of a phospholipid in the interfacial region and m(j) the number of phospholipids in the interfacial region of a liquid cluster of j residues. Equation 106 cannot be directly evaluated since the dependence of m(j) on j is unknown; therefore, an alternative procedure was developed.

The previous equation can be rewritten as

$$\Omega_f = \sigma_{(T)} \sum_{j=1}^{\infty} e^{-j\alpha} \tag{107}$$

where $\sigma_{(T)}$ is a phenomenological parameter defined in such a way that Equations 107 and 108 are identical. $\sigma_{(T)}$ can be considered as an effective, temperature-dependent, cooperative-interaction parameter. The average size of liquid crystal clusters, $\langle \ell_f \rangle$, is, then,

$$\langle \ell_f \rangle = - \frac{\partial \ln \Omega_f}{\partial \alpha}_{\alpha_o} \tag{108}$$

$$= \frac{Z}{Z-1} - \frac{\partial \ln \sigma_{(T)}}{\partial \alpha}_{\alpha_o} \tag{109}$$

In this expression, the first term on the right-hand side is equal to the average size of liquid crystal clusters without including the interfacial region, and the second term represents the average number of phospholipids at the interphase region per cluster. Therefore,

$$\langle \ell_f \rangle = \frac{Z}{z-1} + \langle \ell_{fg} \rangle \tag{110}$$

where $\langle \ell_{fg} \rangle$ is the number of phospholipids surrounding a liquid cluster of $z/(z-1)$ molecules; for convenience, this latter quantity will be called $\langle \ell_{ff} \rangle$. This is the term directly obtained from the experimental data and is the one plotted in Figures 23 and 24.

Several conclusions regarding the transition mechanism of multilamellar DPPC liposomes in the absence and in the presence of halothane can be drawn from the results summarized in Figures 23 and 24. First, the transition is less cooperative in the presence of halothane. Over the entire transition interval, the average size of gel and liquid clusters is greater in the absence of the anesthetic. At the transition midpoint, the average cluster size is about 250 residues, whereas, in the presence of halothane, it is only 80 residues. This decrease in cluster size after addition of the anesthetic is accompanied by an increase in the number of clusters.

The total number of clusters is always maximal at the transition midpoint. At comparable degrees of melting, there are more clusters in the DPPC-halothane system than in the pure DPPC. This increase in the number of clusters is accompanied by an increase in the number of gel-liquid neighbors and, therefore, in the amount of lipids at interfacial regions. This quantity, the number of residues at the gel-liquid boundaries, is proportional to the quantity $\langle \ell_{fg} \rangle$ of Equation 110 and can be estimated from our experimental knowledge of $\langle \ell_{ff} \rangle$. Freire[26] has calculated the fraction of phospholipids at the interface region, assuming a circular geometric shape of the liquid crystalline clusters. Although this assumption with regard to shape is approximate, changes in geometry do not affect the results of the calculation substantially.

The results of Freire[26] constitute the first application of this theory to the study of phospholipid bilayer membranes. It has been demonstrated that scanning calorimetry can, in principle, provide not only the magnitude of the thermodynamic parameters associated with the transition but also a complete statistical thermodynamic description of the system, from which the configurational state of the bilayer could be inferred at any degree of melting. It is anticipated that further studies of this nature relating the various statistical mechanical parameters and changes therein to specific functions and perturbations of model membranes will enhance our overall understanding of such systems.

CONCLUDING REMARKS

Until recently, the use of scanning calorimetry for the study of macromolecular systems

has been limited, as has been pointed out. The goal of such studies has been mainly to provide estimates of the overall enthalpy change for a transition. One exception to this statement is the work of Privalov and co-workers, who have attempted to decompose, in an operational way, the distinct sequential transitions of transfer ribonucleic acids. It now appears that the excess heat capacity function can provide a great deal more information of the thermodynamic nature of complex transitions if the data are properly analyzed. An outline of the appropriate procedures, as applied to a few specific systems, has been provided in this study.

The general application of the described analytical techniques depends upon the attainment of precise and accurate excess heat-capacity data. The mathematical procedures involved in this analysis appear to be sound and should not produce artifacts in the computed results. The resolving power of the technique for cases of discrete, sequential transitions will be determined by the magnitude of the thermodynamic changes at each step and the precision of the data. In fact, it is the latter which is most important.

In the case of cooperative transitions of large, homogeneous systems, the ability to evaluate the partition function of the system allows the calculations of distribution functions as described. While such calculations are independent of assumed models, the interpretation of q in molecular terms must still be done within the context of specific models. The analysis has not, as yet, been extended to finite systems or systems containing more than one chemical component. However, the potential for the analysis of such systems exists, and applications in this area in the not too distant future are to be anticipated.

It is obvious that the excess enthalpy function obtained from precise calorimetric data is the appropriate one to use for this analysis. However, in many cases, it may be possible to analyze systems in which the overall transition is monitored by noncalorimetric techniques (e.g., changes in absorption). This can be done if the monitoring parameter is directly proportional to the excess enthalpy change. Knowing the total enthalpy change, one could, then, transform the "degree of progress" curve into the excess enthalpy function. This does not, of course, obviate the need to have the calorimetrically determined enthalpy change but reduces the requirement of the need for a heat-capacity calorimeter which can precisely define the excess heat capacity as a function of temperature.

The biological or biochemical usefulness of the technique described will become most obvious when functional correlations with changes in thermodynamic parameters of these complex transition curves can be made. For example, if changes in specific functions of tRNA can be correlated with specific transitions or if changes in membrane functions can be correlated with changes in the degree of cooperative interaction, then one will understand in more detail the thermodynamic control of some specific biochemical functions. Until that time, the procedures described herein should provide a better understanding of the statistical thermodynamic behavior of interacting biological macromolecular systems.

ACKNOWLEDGMENTS

We wish to thank several colleagues, including Dr. Donald B. Mountcastle, Dr. Maurice Eftink, Vincent Chau, and Guillermo Romero for their many helpful comments during the course of this work. Research from this laboratory described herein was supported by grants from the National Institutes of Health (GM-20637-05, P17 AM-17042-03), the National Science Foundation (PCM75-23245-A01), and the American Cancer Society (BC-240-01). The skillful help of Cynthia Annunziata during the preparation of this manuscript is appreciated

ARTICLES REVIEWED

Freire, E. and Biltonen, R., Statistical mechanical deconvolution of thermal transitions in macromolecules. I. Theory and application to homogeneous systems, *Biopolymers*, 17, 463, 1978.

Freire, E. and Biltonen, R., Statistical mechanical deconvolution of thermal transitions in macromolecules. II. General treatment of cooperative phenomena, *Biopolymers*, 17, 481, 1978.

Freire, E. and Biltonen, R., Statistical mechanical deconvolution of thermal transitions in macromolecules. III. Application to double-stranded single-stranded transitions of nucleic acids, *Biopolymers,* 17, 497, 1978.

Hinz, H., Filiminov, V., and Privalov, P., Calorimetric studies on melting of $tRNA^{Phe}$ (yeast), *Eur. J. Biochem.,* 72, 79, 1977.

Hinz, H. and Sturtevant, J., Calorimetric studies of dilute aqueous suspensions of bilayers formed from synthetic L-α-lecithins, *J. Biol. Chem.,* 247, 6071, 1972.

Neumann, E. and Ackermann, T., Thermodynamic investigation of the helix-coil transition of a polyribonucleotide system, *J. Phys. Chem.,* 73, 2170, 1969.

Privalov, P., Filiminov, V., Venkstern, T., and Bayev, T., A calorimetric investigation of $tRNA^{val}$ melting, *J. Mol. Biol.,* 97, 279, 1975.

REFERENCES

1. **Privalov, P., Plotnikov, V., and Filiminov, V.,** Precision scanning microcalorimeter for the study of liquids, *J. Chem. Thermodyn.,* 7, 41, 1975.
2. **Sturtevant, J.,** Some applications of calorimetry in biochemistry and biology, in *Annual Review of Biophysics and Bioengineering,* Vol. 3, Mullins, L., Ed., Annual Reviews, Inc., Palto Alto, California, 1974, 35.
3. **McNaughton, J. and Mortimer, C.,** Differential scanning calorimetry, in *Physical Chemistry Series Two,* Vol. 10, Skinner, H., Ed., Butterworths, London, 1975, 1.
4. **Calvet, E. and Prat, H.,** *Recent Progress in Microcalorimetry,* Pergamon Press, New York, 1963.
5. **Ackermann, T.,** The calorimeters: adiabatic calorimeters, in *Biochemical Microcalorimetry,* Brown, H. D., Ed., Academic Press, New York, 1969, 235.
6. **Jackson, W. and Brandts, J.,** Thermodynamics of protein denaturation. A calorimetric study of the reversible denaturation of chymotrypsinogen and conclusions regarding the accuracy of the two-state approximation, *Biochemistry,* 9, 2294, 1970.
7. **Gill, S. and Beck, K.,** Differential heat capacity calorimeter for polymer transition studies, *Rev. Sci. Instrum.,* 36, 274, 1965.
8. **Privalov, P. L.,** Thermal investigations of biopolymers solutions and scanning microcalorimetry, *FEBS Lett.,* 40, 5140, 1974.
9. **Danforth, R., Krakauer, H., and Sturtevant, J.,** Differential calorimetry of thermally induced processes in solution, *Rev. Sci. Instrum.,* 38, 484, 1967.
10. **Ross, P. and Goldberg, R.,** A scanning microcalorimeter for thermally induced transitions in solution, *Thermochim. Acta,* 10, 143, 1974.
11. **Suurkuusk, J., Lentz, B., Barenholz, Y., Biltonen, R., and Thompson, T.,** A calorimetric and fluorescent probe study of the gel-liquid crystalline phase transition in small single-lamellar dipalmitoylphosphatidylcholine vesicles, *Biochemistry,* 15, 1393, 1976.
12. **Lumry, R., Biltonen, R., and Brandts, J.,** Validity of the "two-state" hypothesis for conformational transitions of proteins, *Biopolymers,* 4, 917, 1966.
13. **Privalov, P., Ptitsyn, O., and Birshtein, T.,** Determination of stability of the DNA double helix in an aqueous medium, *Biopolymers,* 8, 559, 1969.
14. **Ackermann, T. and Neumann, E.,** Experimental thermodynamics of the helix-random coil transition. I. Influence of polymer concentration and solvent composition in the PBG-DCA-EDC system, *Biopolymers,* 5, 649, 1967.
15. **Zimm, B. and Bragg, J.,** Theory of the phase transition between helix and random coil in polypeptide chains, *J. Chem. Phys.,* 31, 526, 1959.
16. **Neumann, E. and Ackermann, T.,** Thermodynamic investigation of the helix-coil transition of a polyribonucleotide system, *J. Phys. Chem.,* 73, 2170, 1969.
17. **Ackermann, T.,** Physical states of biomolecules: calorimetric study of helix-random coil transitions in solution, in *Biochemical Microcalorimetry,* Brown, H. D., Ed., Academic Press, New York, 1969, 121.
18. **Privalov, P. and Khechinashvili, N.,** A thermodynamic approach to the problem of stabilization of globular protein structure: a calorimetric study, *J. Mol. Biol.,* 86, 665, 1974.
19. **Brandts, J., Jackson, W., and Yao-Chung Ting, T.,** A calorimetric study of the thermal transitions of three specific transfer ribonucleic acids, *Biochemistry,* 13, 3595, 1974.
20. **Privalov, P., Filiminov, V., Venkstern, T., and Bayev, A.,** A calorimetric investigation of $tRNA_1^{val}$ melting, *J. Mol. Biol.,* 97, 279, 1975.
21. **Hinz, H., Filiminov, V., and Privalov, P.,** Calorimetric studies on melting of $tRNA^{Phe}$ (yeast), *Eur. J. Biochem.,* 72, 79, 1977.
22. **Huang, C.,** Studies of phosphatidylcholine vesicles. Formation and physical characteristics, *Biochemistry,* 8, 344, 1969.
23. **Hinz, H. and Sturtevant, J.,** Calorimetric studies of dilute aqueous suspensions of bilayers formed from synthetic L-α-Lecithins, *J. Biol. Chem.,* 274, 6071, 1972.

24. **Mabrey, S. and Sturtevant, J.,** Investigation of phase transitions of lipids and lipid mixtures by high sensitivity differential scanning calorimetry, *Proc. Natl. Acad. Sci. U.S.A.*, 73, 3862, 1976.
25. **Barenholz, Y., Suurkuusk, J., Mountcastle, D., Thompson, T., and Biltonen, R.,** A calorimetric study of the thermotropic behavior of aqueous dispersions of natural and synthetic sphyngomyelins, *Biochemistry*, 15, 2441, 1976.
26. **Freire, E.,** Statistical Thermodynamics of Conformational Transitions in Macromolecules, Ph.D. dissertation, University of Virginia, 1977.
27. **Freire, E. and Biltonen, R.,** Statistical mechanical deconvolution of thermal transitions in macromolecules. I. Theory and applications to homogeneous systems, *Biopolymers*, 17, 463, 1978.
28. **Bode, D., Schernau, V., and Ackermann, T.,** Calorimetric investigation of the helix-coil conversion of phenylalanine-specific transfer ribonucleic acid, *Biophys. Chem.*, 1, 214, 1974.
29. **Freire, E. and Biltonen, R.,** Thermodynamics of transfer ribonucleic acids: the effect of sodium on the thermal unfolding of yeast $tRNA^{Phe}$, *Biopolymers*, 17, 1257, 1978.
30. **Crothers, D., Cole, P., Hilbers, C., and Shulman, R.,** The molecular mechanism of thermal unfolding of *Escherichia coli* formylmethionine transfer RNA, *J. Mol. Biol.*, 87, 63, 1974.
31. **Riesner, D., Maas, G., Thiebe, R., Philippsen, P., and Zachau, H.,** The conformational transitions in yeast $tRNA^{Phe}$ as studied with $tRNA^{Phe}$ fragments, *Eur. J. Biochem.*, 36, 76, 1973.
32. **Freire, E. and Biltonen, R.,** Statistical mechanical deconvolution of thermal transitions in macromolecules. II. General treatment of cooperative phenomena, *Biopolymers*, 17, 481, 1978.
33. **Thompson, C. J.,** *Mathematical Statistical Mechanics*, The Macmillan Company, New York, 1972, chap. 3.
34. **Lifson, S. and Zimm, B.,** Simplified theory of the helix-coil transition in DNA based on a grand partition function, *Biopolymers*, 1, 15, 1963.
35. **Sture, K. and Nordholm, J.,** A new analytic solution for the Zwanzig-Lauritzen model of polymer chain folding, *J. Stat Phys.*, 9, 235, 1973.
36. **Sture, K., Nordholm, J., and Rice, S.,** Phase transitions and end effects in models of biopolymers, *J. Chem. Phys.*, 59, 5605, 1973.
37. **Lifson, S.,** Partition function of linear-chain molecules, *J. Chem. Phys.*, 40, 3705, 1964.
38. **Poland, D. and Scheraga, H.,** *Theory of Helix-coil Transitions in Biopolymers*, Academic Press, New York, 1970, chap. 7.
39. **Applequist, J.,** Higher-order phase transitions in two-stranded macromolecules, *J. Chem. Phys.*, 50, 600, 1969.
40. **Freire, E. and Biltonen, R.,** Statistical mechanical deconvolution of thermal transitions in macromolecules. III. Application to double-stranded single-stranded transitions of nucleic acids, *Biopolymers*, 17, 497, 1978.
41. **Blake, R.,** Helix-coil equilibria of Poly(rA) · Poly(rU), *Biophys. Chem.*, 1, 24, 1973.
42. **Vibina, J. and Waugh, J.,** Proton-enhanced ^{13}C nuclear magnetic resonance of lipids and biomembranes, *Proc. Natl. Acad. Sci. U.S.A.*, 71, 5062, 1974.
43. **Levine, Y. and Wilkins, M.,** Structure of oriented lipid bilayers, *Nature (London) New Biol.*, 230, 69, 1971.
44. **Nagle, J.,** Lipid bilayer phase transition: density measurements and theory, *Proc. Natl. Acad. Sci. U.S.A.*, 70, 3443, 1973.
45. **Jackson, M.,** A β-coupled gauch-kink description of the lipid bilayer phase transition, *Biochemistry*, 15, 2555, 1976.
46. **Mountcastle, D., Halsey, M., and Biltonen, R.,** The effects of anesthetics and pressure on the thermotropic behavior of multilamellar dipalmitoylphosphatidylcholine liposomes, *Proc. Natl. Acad. Sci. U.S.A.*, in press.
47. **Tsong, T., Hearn, R., Wrathall, D., and Sturtevant, J.,** A calorimetric study of thermally induced conformational transitions of Ribonuclease A and certain of its derivatives, *Biochemistry*, 1, 2666, 1970.
48. **Suurkuusk, J., Alvarez, J., Freire, E., and Biltonen, R.,** Calorimetric determination of the heat capacity changes associated with the conformational transitions of polyriboadenylic acid and polyribouridylic acid, *Biopolymers*, 16, 2641, 1977.
49. **Krakauer, H. and Sturtevant, J.,** Heats of the helix-coil transitions of the Poly A-Poly U complexes, *Biopolymers*, 6, 491, 1968.
50. **Klump, H. and Ackermann, T.,** Experimental thermodynamics of the helix-random coil transition. IV. Influence of the base composition of DNA on the transition enthalpy, *Biopolymers*, 10, 513, 1971.
51. **Scheffler, I. and Sturtevant, J.,** Thermodynamics of the helix-coil transition of the alternating copolymer of deoxyadenylic acid and deoxythymidylic acid, *J. Mol. Biol.*, 42, 577, 1969.
52. **Bloomfield, V., Crothers, D., and Tinoco, I.,** *Physical Chemistry of Nucleic Acids*, Harper and Row, New York, 1974.
53. **Kauzmann, W.,** Some factors in the interpretation of protein denaturation, in *Advances in Protein Chemistry*, Vol. 14, Academic Press, New York, 1959, 1.
54. **Lumry, R. and Biltonen, R.,** Thermodynamic and kinetic aspects of protein conformations in relation to physiological function, in *Structure and Stability of Biological Macromolecules*, Timasheff, S. N. and Fasman, G. D., Eds., Marcel Dekker, New York, 1969, 65.
55. **Brandts, J. F.,** Conformational transitions of proteins in water and aqueous mixtures, in *Structure and Stability of Biological Macromolecules*, Timasheff, S. N. and Fasman, G. D., Marcel Dekker, New York, 1969, 213.
56. **Tsong, T. Y. and Kanehisa, M. I.,** Relaxation phenomena in aqueous dispersions of synthetic lecithins, *Biochemistry*, 16, 2674, 1977.
57. **Lentz, B., Freire, E., and Biltonen, R.,** Fluorescence and calorimetric studies of phase transitions in phosphatidylcholine multilayers: kinetics of the pretransition, *Biochemistry*, in press.
58. **Applequist, J.,** Macromolecular cooperative phenomena, in *Conformation of Biopolymers*, Vol. 1, Ramachandran, G. N., Ed., Academic Press, New York, 1967, 403.